© 2016. Published by The Company of Biologists Ltd | Development (2016) 143, 1859-1873 doi:10.1242/dev.133215

mTor signaling is required for the formation of proliferating Müller glia-derived progenitor cells in the chick retina

Christopher P. Zelinka*, Leo Volkov, Zachary A. Goodman, Levi Todd, Isabella Palazzo, William A. Bishop and Andy J. Fischer‡

ABSTRACT

We investigate the roles of mTor signaling in the formation of Müller glia-derived progenitor cells (MGPCs) in the chick retina. During embryonic development, pS6 (a readout of active mTor signaling) is present in early-stage retinal progenitors, differentiating amacrine and ganglion cells, and late-stage progenitors or maturing Müller glia. By contrast, pS6 is present at low levels in a few scattered cell types in mature, healthy retina. Following retinal damage, in which MGPCs are known to form, mTor signaling is rapidly activated in Müller glia. Inhibition of mTor in damaged retinas prevented the accumulation of pS6 in Müller glia and reduced numbers of proliferating MGPCs. Inhibition of mTor had no effect on MAPK signaling or on upregulation of the stem cell factor Klf4, whereas Pax6 upregulation was significantly reduced. Inhibition of mTor potently blocked the MGPC-promoting effects of Hedgehog, Wnt and glucocorticoid signaling in damaged retinas. In the absence of retinal damage, insulin, IGF1 and FGF2 induced pS6 in Müller glia, and this was blocked by mTor inhibitor. In FGF2-treated retinas, in which MGPCs are known to form, inhibition of mTor blocked the accumulation of pS6, the upregulation of Pax6 and the formation of proliferating MGPCs. We conclude that mTor signaling is required, but not sufficient, to stimulate Müller glia to give rise to proliferating progenitors, and the network of signaling pathways that drive the formation of MGPCs requires activation of mTor.

KEY WORDS: Müller glia, mTor, Progenitor, Regeneration, Retina

INTRODUCTION

Glial cell function in the retina is crucial to maintain normal vision. Glial cells are involved in the pathology of many different retinal diseases and glial dysfunction alone can compromise vision. The signaling pathways that coordinate the functions of retinal glia remain poorly understood. One of the signaling pathways that may influence retinal glia is the mTor cell signaling pathway, which is involved in cellular processes including growth and proliferation. During the development of the nervous system, mTor signaling is important for the initiation of neural differentiation (Fishwick et al., 2010). However, little is known about mTor signaling in the developing or mature retina. The purpose of the current study was to investigate the roles of mTor signaling in Müller glia and during the formation of Müller glia-derived progenitor cells (MGPCs).

Department of Neuroscience, College of Medicine, The Ohio State University, 4190 Graves Hall, 333 West 10th Avenue, Columbus, OH 43210-1239, USA.
*Present address: Department of Biological Science, Florida State University, Tallahassee, FL 32306, USA.

‡Author for correspondence (andrew.fischer@osumc.edu)

A.J.F., 0000-0001-6123-7405

Received 2 December 2015; Accepted 4 April 2016

Müller glia are the major type of support cell in the retina and, in lower vertebrates, can act as a source of neural progenitors. The Müller glia are common to the eyes of all vertebrate classes and are the only type of retinal glia that is derived from embryonic neuroepithelial stem cells. In several vertebrate classes the Müller glia are capable of de-differentiating, proliferating and acquiring a progenitor-like state in response to acute retinal injury (Bernardos et al., 2007; Fausett and Goldman, 2006; Fischer and Reh, 2001; Karl et al., 2008; Ooto et al., 2004) or in response to exogenous growth factors (Fischer et al., 2002; Kassen et al., 2009; Nelson et al., 2013; Wan et al., 2012). Müller glia have been identified as the cellular source of retinal regeneration in zebrafish (Bernardos et al., 2007; Fausett and Goldman, 2006), birds (Fischer and Reh, 2001) and rodent models (Karl et al., 2008; Ooto et al., 2004). Müller glia in the fish retina have an extraordinary capacity to regenerate retinal neurons. By comparison, Müller glia in birds have a limited capacity to regenerate neurons, and this capacity is further diminished in rodents.

Müller glia are distinctly different from progenitor cells based on cellular functions and phenotype. Interestingly, rodent Müller glia share a significant, nearly 70%, overlap of transcriptomes with retinal progenitors (Blackshaw et al., 2004; Roesch et al., 2008). In fish and bird Müller glia, during the transition to a progenitor-like phenotype, transcription factors such as Ascl1a, Klf4, Pax6, Chx10 and Six3 are upregulated and proliferation occurs (reviewed by Fischer and Bongini, 2010; Gallina et al., 2014a). In response to sufficient levels of neuronal damage, numerous Müller glia de-differentiate and re-enter the cell cycle (Fischer and Reh, 2001; Fischer et al., 2009a). In the bird retina *in vivo*, numerous Müller glia undergo a single round of division; these cells continue to proliferate when they are dissociated and grown in culture (Fischer and Reh, 2001). In all vertebrate models, the proliferation of the Müller glia is an integral step toward becoming progenitor cells (Fischer, 2005; Fischer and Reh, 2003; Gallina et al., 2014a,b).

In fish, birds and mammals, there is a confluence of cell signaling pathways that influence the formation of MGPCs. These pathways are known to include MAPK (Fischer et al., 2002, 2009b; Wan et al., 2012), Wnt/β-catenin (Gallina et al., 2016; Osakada et al., 2007; Ramachandran et al., 2011), Notch (Conner et al., 2014; Ghai et al., 2010; Hayes et al., 2007; Raymond et al., 2006), Hedgehog (Sherpa et al., 2014; Todd and Fischer, 2015), glucocorticoid (Gallina et al., 2014b), Jak/Stat (Nelson et al., 2012; Wan et al., 2014) and TGFβ/Smad (Lenkowski et al., 2013) signaling. The identification of the secreted factors and signaling pathways that stimulate Müller glia without further damaging retinal neurons is crucial to harnessing the neurogenic potential of these glia. The purpose of the studies described herein is to investigate how the mTor signaling pathway influences the formation of proliferating MGPCs.

Development (2016) 143, 1859-1873 doi:10.1242/dev.133215

RESULTS

mTor signaling in the developing retina

We assayed for mTor activity by immunofluorescence labeling for phosphorylated S6 (pS6). Activated mTor, as part of the mTORC1 complex, phosphorylates and activates 70S6K, which in turn phosphorylates and activates S6, a component of the 40S ribosomal subunit (reviewed by Sawyers, 2008; Dazert and Hall, 2011). We assayed for pS6 using polyclonal and monoclonal antibodies that were raised to a synthetic phospho-peptide corresponding to residues surrounding Ser240 and Ser244 at the C-terminus of human ribosomal protein S6 (RPS6). The 40 amino acids at the C-terminus of chick S6 are identical to the human sequence. The specificity of the antibodies was supported by findings that both polyclonal and monoclonal pS6 antibodies produced identical patterns of labeling, and that upregulation of pS6, as detected with the antibodies, was blocked by mTor inhibitors (see Fig. 3A,E, Fig. 4A,F, Fig. 7E-K, Fig. S1A,B).

pS6 was detected in chick E4 retinas in differentiating ganglion cells and fusiform cells (Fig. 1A), reminiscent of postmitotic neurons migrating away from the ventricular surface toward the prospective ganglion cell layer (GCL) (Fischer and Omar, 2005; McCabe et al., 1999). At E6, pS6 was prevalent in fusiform cells found predominantly within the vitread half of the prospective retina (Fig. 1B). In central regions of E4 and E6 retinas, pS6 was found in maturing neurons that were positive for HuD/C, but not neurofilament (Fig. 1J,K). In peripheral regions of E6 retina, pS6 was present in cells that preceded the front of differentiation, and pS6 was colocalized to neurofilament-positive cells (Fig. 1N). The front of differentiation is the zone of retina where cells first express markers of neuronal differentiation, such as neurofilament, which spreads from central to peripheral regions of the retina as development proceeds (McCabe et al., 1999). At E7 through E10, pS6 was detected in Sox2-positive progenitors and/or immature Müller glia and in Sox2-positive mitotic figures at the ventricular surface of the retina (Fig. 1C-F,L-P). At E12 through E16, pS6 was seen in a few presumptive amacrine and ganglion cells, and a few presumptive Müller glia based on the size, shape and position of the somata within the retina (Fig. 1G-I).

Levels of pS6 were relatively low in mature, normal retinas at post-hatch day (P) 7 (Fig. 2A), and this pattern of labeling remained unchanged through P21 (not shown). pS6 was not detected in Sox2-expressing Müller glia in the inner nuclear layer (INL) in central regions of the retina (Fig. 2A). In addition, pS6 was present in a few Brn3a-positive ganglion cells (Fig. 2B,C) and oligodendrocytes that express transferrin-binding protein (TFBP) (Fig. 2D). Immunoreactivity was observed in SV2-positive axon

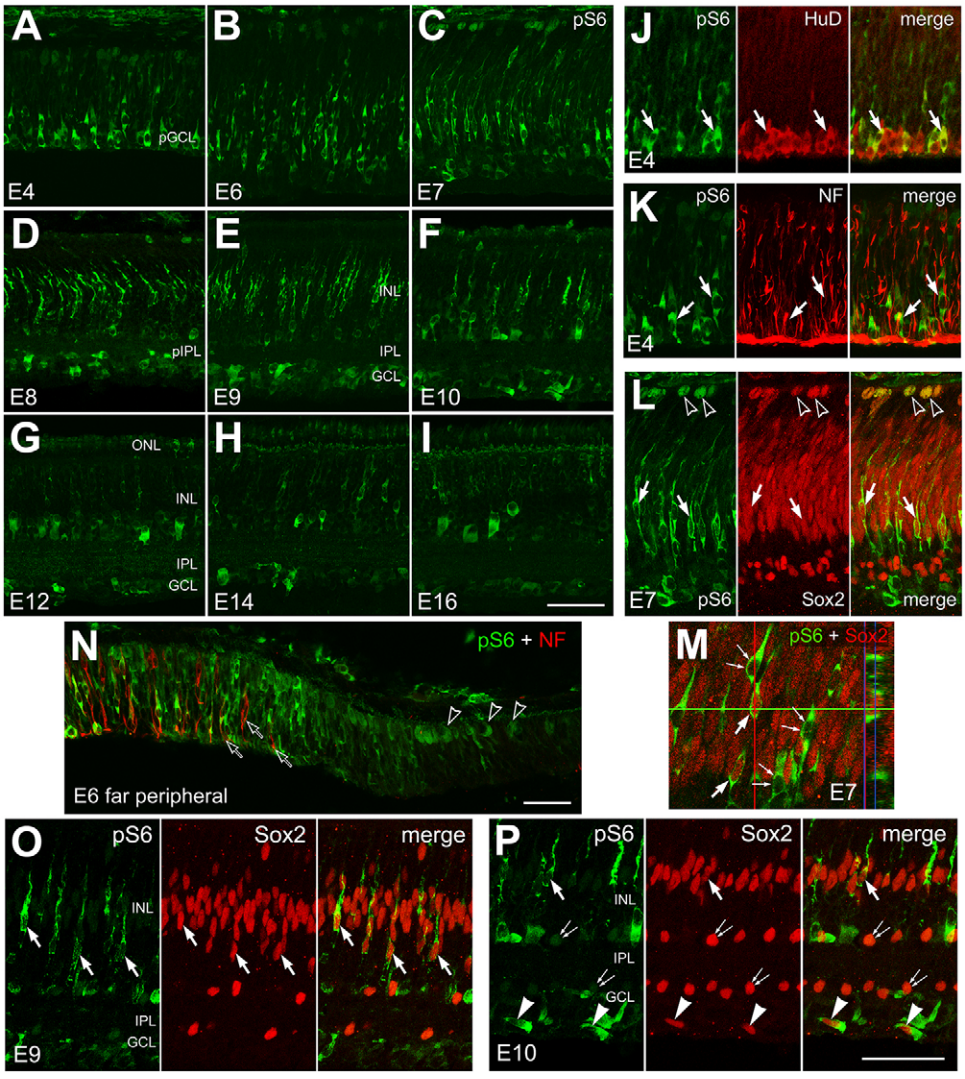

Fig. 1. pS6 in developing retina. Sections of the retina were obtained from chick embryos at E4 (A,J,K), E6 (B,N), E7 (C,L,M), E8 (D), E9 (E,O), E10 (F,P), E12 (G), E14 (H) and E16 (I). Sections were labeled with antibodies to pS6 (green), HuD/C (red; J), neurofilament (NF) (red; K,N), and Sox2 (red; L,M,O,P). Confocal microscopy was used to obtain *z*-stacks of images or produce orthogonal projections (M). Arrows indicate cells double-labeled for pS6 and HuD/C or Sox2; arrowheads indicate presumptive NIRG cells; open arrowheads indicate presumptive mitotic cells; and open arrows indicate neurofilament^{+}/pS6^{-} cells. The small double-arrows in M indicate pS6-positive/Sox2-negative cells, and in P indicate Sox2-positive orthotopic and ectopic amacrine cells. ONL, outer nuclear layer; INL, inner nuclear layer; IPL, inner plexiform layer; GCL, ganglion cell layer; NFL, nerve fiber layer; p, presumptive. Scale bars: 50 µm (in I for A-I; in P for J-M,O,P).

Development (2016) 143, 1859-1873 doi:10.1242/dev.133215

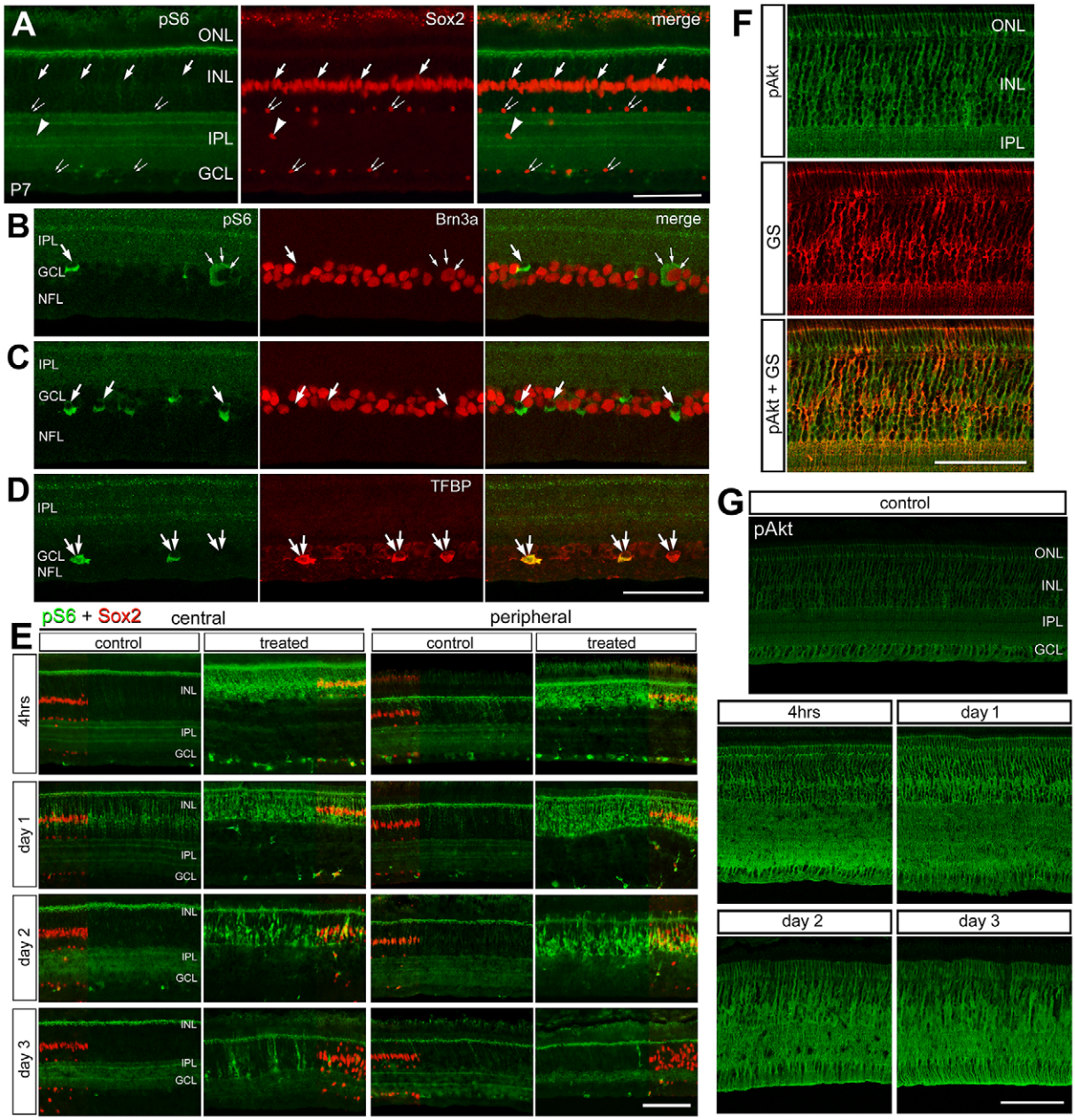

Fig. 2. pS6 and pAkt in mature undamaged retina and following NMDA-induced damage. Retinal sections were obtained from central regions of P7 chick retinas (A-D) and at different time-points after NMDA treatment (E-G). Sections were labeled with antibodies to pS6, Sox2 (A,E), Brn3a (B,C), TFBP (D), glutamine synthetase (GS; F) and pAkt (F,G). Eyes were injected with 1 µmol of NMDA at P7 and retinas were harvested 2 h, 4 h, 1, 2 or 3 days later. Retinal sections were obtained from central and peripheral regions (E). Sox2 is included as a partial field overlay to indicate the nuclei of Müller glia in the center of the INL (E). The small round $Sox2^{+}/pS6^{-}$ nuclei in the INL and GCL are those of cholinergic amacrine cells (Ghai et al., 2009). Arrows indicate $pS6^{+}/Brn3a^{-}$ cells (B,C); small arrows indicate a ganglion cell double-labeled for pS6 and Brn3a (B); and double-arrows indicate $TFBP^{+}$ oligodendrocytes (D). TFBP, transferrin binding protein. Scale bars: 50 µm (in D for B-D).

terminals in the outer plexiform layer (OPL) (not shown). This immunoreactivity is likely to be non-specific given that this pattern of labeling is not perturbed by treatments that influence cell signaling (see below).

Levels of pS6 in damaged retinas

We assayed for levels of pS6 in retinas damaged by *N*-methyl-D-aspartate (NMDA), which is known to destroy many inner retinal neurons and stimulate the formation of proliferating MGPCs (Fischer and Reh, 2001; Fischer et al., 1998a). In control eyes 1 day after injection of vehicle, there was a noticeable accumulation of pS6 in Sox2-positive Müller glia in both central and peripheral regions of the retina (Fig. 2E). Levels of pS6 in vehicle-treated retinas were reduced to levels seen in untreated retinas at 2 and 3 days after treatment (Fig. 2E). The pS6 observed in Müller glia in control retinas suggests that there might be contralateral effects related to damage, given that levels of cell death are maximal 24 h after NMDA treatment (Fischer et al., 1998a) and vehicle-treated retinas, where the contralateral retinas were undamaged, did not exhibit elevated pS6 at any time (see below). By comparison, there was a substantial upregulation of pS6 in Sox2-positive Müller glia in the INL at 4 h, 1 and 2 days after NMDA treatment (Fig. 3A). At

Development (2016) 143, 1859-1873 doi:10.1242/dev.133215

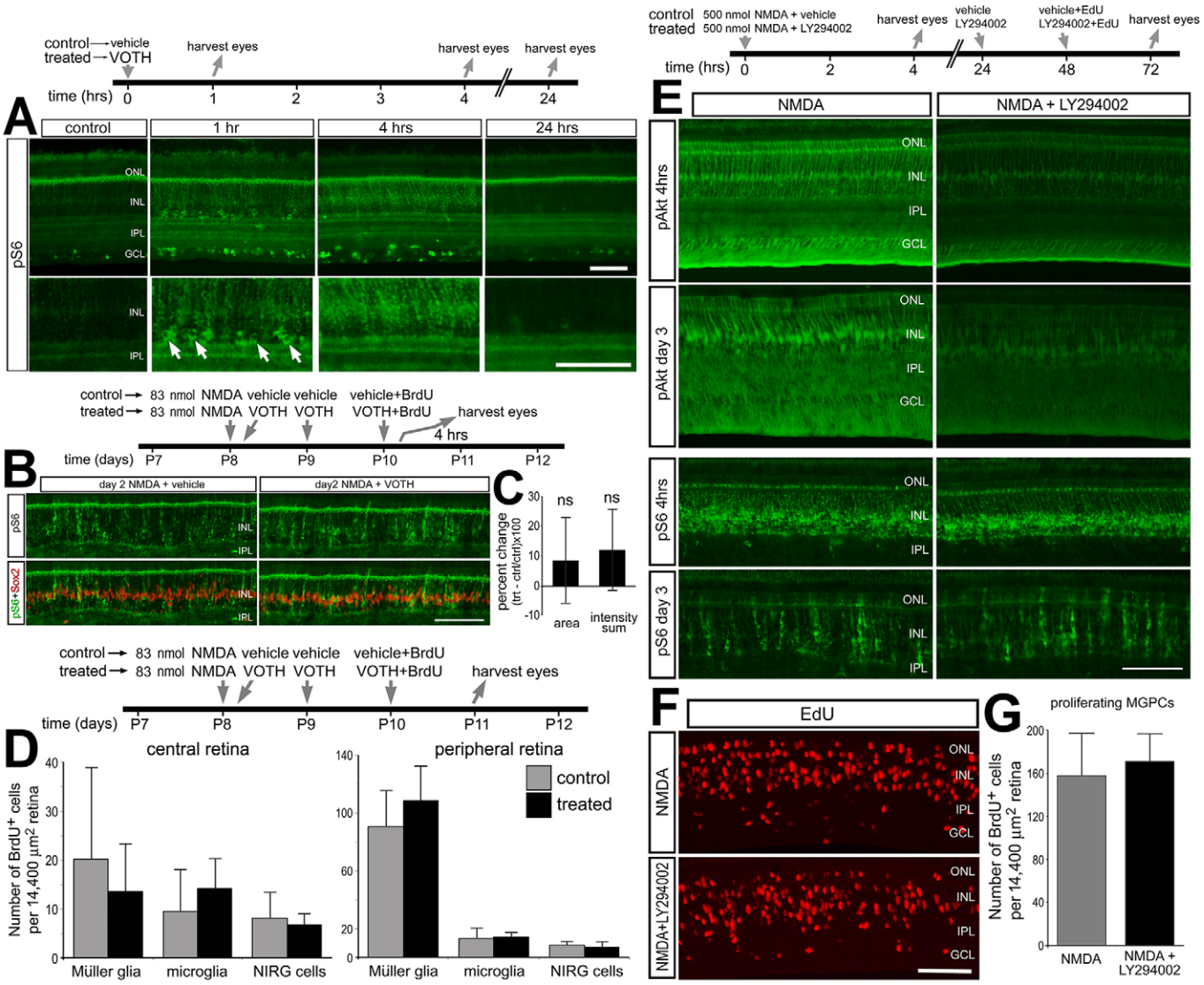

Fig. 3. PI3K, PTEN and mTor signaling in damaged retinas. (A) Retinas were obtained from eyes that were injected with vehicle (control) or the PTEN inhibitor VOTH (treated) and harvested 1 h, 4 h or 24 h later. (B-G) VOTH or the PI3K inhibitor LY294002 was applied at different times after a low (83 nmol) or high (500 nmol) dose of NMDA, BrdU or EdU applied to label proliferating cells, and retinas harvested at different times after treatment. Retinal sections were labeled with antibodies to pS6 (A,B,E), Sox2 (B), pAkt (E) or EdU (F). The lower panels in A are enlarged (2.2×) fields of view to illustrate the accumulation of pS6 in presumptive amacrine cells (arrows). (C) The mean (±s.d.; n=5) area and intensity sum of pS6 in the INL in control and treated retinas. Significance of difference (ns, not significant) was determined by using a Mann–Whitney U-test. Numbers of proliferating Müller glia/MGPCs ($BrdU^+/Sox9^+/Nkx2.2^-$), microglia ($BrdU^+/CD45^+$) and NIRG cells ($BrdU^+/Sox9^+/Nkx2.2^+$) were determined for central and peripheral regions of the retina. (D) The mean (±s.d.; n=8) number of proliferating Müller glia, NIRG cells and microglia in central and peripheral regions of control and treated retinas. (G) The mean (±s.d.; n=6) number of proliferating Müller glia/MGPCs in peripheral retina. No significant differences were found using an unpaired, two-tailed t-test. Scale bars: 50 µm.

3 days after NMDA treatment, pS6 remained elevated in a few scattered Müller glia and/or MGPCs in central and peripheral regions of the retina, but was decreased compared with earlier time points (Fig. 2E).

In undamaged retinas, we detected pAkt in Müller glia (Fig. 2F), suggesting that PI3K signaling might normally be active in mature Müller glia. pAkt was upregulated in Müller glia at 4 h following NMDA treatment, and remained elevated through 24, 48 and 72 h after treatment (Fig. 2G). Unlike the patterns of pS6 immunolabeling, pAkt was uniformly upregulated across central and peripheral regions of the retina (not shown). In summary, upregulation of pS6 is transient and pAkt is sustained and predominant in Müller glia/MGPCs following NMDA treatment, indicating that acute retinal damage results in the activation of PI3K and mTor signaling in the Müller glia before and during the transition to a progenitor-like state.

Inhibition of PI3K and PTEN

We examined the effects of a PTEN inhibitor (VO-OHpic trihydrate, VOTH) and a PI3K inhibitor (LY2942002) on Akt and mTor signaling in the retina. Inhibition of PTEN is expected to facilitate mTor signaling, whereas inhibition of PI3K is expected to suppress mTor signaling (Dazert and Hall, 2011; Zoncu et al., 2011). To assess the specificity of the PTEN inhibitor we assayed for levels of pS6 and determined whether there were any off-target effects on the MAPK pathway. Levels of cFos, pCREB and pERK were not affected by VOTH (not shown). At 1 h after VOTH treatment, there was an accumulation of pS6 in Müller glia, some

Development (2016) 143, 1859-1873 doi:10.1242/dev.133215

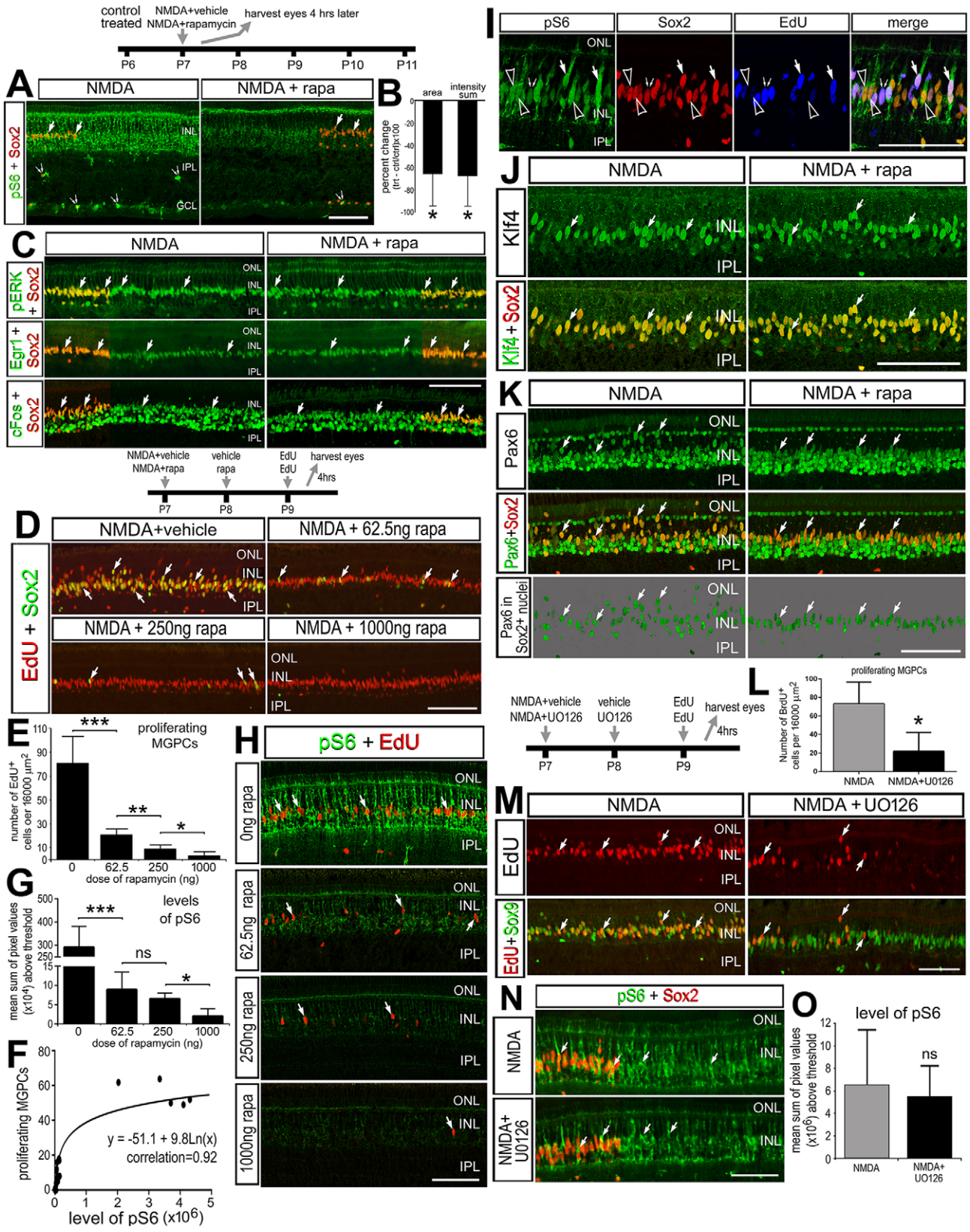

Fig. 4. See next page for legend.

amacrine cells, ganglion cells, and non-astrocytic inner retinal glial (NIRG) cells and/or oligodendrocytes in the inner plexiform layer (IPL) and GCL (Fig. 3A). In the chick retina, NIRG cells are a distinct type of glial cell that migrates into the IPL and GCL from the optic nerve during development (Fischer et al., 2010; Rompani and Cepko, 2010). At 4 h after VOTH treatment, levels of pS6

Development (2016) 143, 1859-1873 doi:10.1242/dev.133215

Fig. 4. Inhibition of mTor with rapamycin following NMDA treatment blocks the accumulation of pS6, but not readouts of MAPK signaling. Retinas were obtained from eyes that were: (A-C) injected with NMDA and vehicle (control) or NMDA and rapamycin (treated) at P7, and harvested 4 h after injection; (D-K) injected at P7 with NMDA and vehicle (control) or NMDA and different doses of rapamycin (treated), vehicle or rapamycin at P8, EdU at P9 and harvested 4 h later to identify cells entering S-phase; or (L-O) injected with NMDA and vehicle (control) or NMDA and UO126 DMSO (treated), vehicle or UO126 at P8, EdU at P9 and harvested 4 h later. Sections of the retina were labeled with antibodies to Sox2 and pS6 (A), Sox2 and pERK1/2, Egr1 or cFos (C), EdU and Sox2 (D), pS6 (H), pS6, Sox2 and EdU (I), Klf4 and Sox2 (J), Pax6 and Sox2 (K), EdU and Sox9 (M), and Sox2 and pS6 (N). Sox2 is included as a partial field overlay to indicate the nuclei of Müller glia in the center of the INL (A,C,N). (B) The mean (±s.d.; n=5) percentage change in the area of pixels above threshold, and the percentage change in the sum of pixel values above threshold. *P<0.01, Mann–Whitney U-test. (E,L) The mean (±s.d.; n≥5) number of BrdU-labeled MGPCs. *P<0.05, *P<0.01, ***P<0.001, ANOVA followed by a two-tailed t-test with Bonferroni correction. (G,O) The mean (±s.d.; n=5) intensity sum for levels of pS6 in the INL. (F) Scatter plot and best-fit semi-log plot illustrating the relationship between levels of pS6 and numbers of proliferating MGPCs with different doses of rapamycin in NMDA-damaged retinas. Arrows indicate the nuclei of Müller glia and small double-arrows indicate the nuclei of NIRG cells. (I) Open arrowheads indicate nuclei labeled for pS6 and Sox2 (not EdU), small arrowheads indicate nuclei labeled for EdU and Sox2 (not pS6), and arrows indicate nuclei labeled pS6, Sox2 and EdU. Scale bars: 50 µm.

appeared further elevated in the Müller glia, whereas levels in amacrine cells appeared reduced (Fig. 3A). Levels of pS6 returned to control levels by 24 h after the injection of VOTH (Fig. 3A). At no time after treatment with VOTH did the contralateral vehicle-treated retinas exhibit elevated levels of pS6.

We tested whether inhibition of PTEN influenced the formation of proliferating MGPCs. Retinas were treated with a relatively low dose of NMDA, followed by treatment with VOTH, and application of BrdU to label proliferating cells. We assayed for proliferation in central retina, where MGPCs tend not to form, and peripheral regions of the retina, where MGPCs are more abundant (Fischer and Bongini, 2010; Fischer and Reh, 2001; Gallina et al., 2014a). Inhibition of PTEN with VOTH in NMDA-damaged retinas failed to influence the proliferation of MGPCs, microglia and NIRG cells in central or peripheral regions of the retina (Fig. 3C,D).

To examine the specificity of the PI3K inhibitor and the pAkt antibody we probed for levels of pAkt following retinal damage and treatment with inhibitor. In NMDA-treated retinas, LY294002 inhibited the accumulation of pAkt, but not of pS6, in Müller glia at 4 h and 3 days after treatment (Fig. 3E). These findings suggest that signaling through PI3K and Akt might not underlie the activation of mTor in NMDA-treated Müller glia. Inhibition of PI3K failed to influence the numbers of proliferating MGPCs in NMDA-damaged retinas (Fig. 3F,G).

Inhibition of mTor

We investigated whether inhibition of mTor with rapamycin influenced the levels of pS6 and the formation of MGPCs. In undamaged retinas, rapamycin had no detectable effects on pS6 levels or cell survival, and did not induce glial reactivity (not shown). Application of rapamycin with NMDA effectively blocked the rapid accumulation of pS6 in Müller glia and inner retinal glia, presumptive microglia and/or NIRG cells in the IPL and GCL (Fig. 4A,B). Similar to pS6, levels of pERK1/2, pCREB, p38 MAPK, cFos and Egr1 are rapidly and transiently upregulated by Müller glia after treatment with NMDA (Fischer et al., 2009b). However, accumulations of pERK1/2, Egr1, cFos (Fig. 4C), pCREB and p38 MAPK (not shown) were unaffected in Müller glia in damaged retinas treated with rapamycin. Similar to the effects of rapamycin, the mTor inhibitor ridaforolimus inhibited the upregulation of pS6 4 h after NMDA treatment (Fig. S1A,B).

We tested whether inhibition of mTor influenced the re-entry of Müller glia into the cell cycle, which is known to begin 2 days after NMDA treatment (Fischer and Reh, 2001). We found that rapamycin significantly reduced the number of Müller glia that proliferated at 2 days after NMDA treatment (Fig. 4D,E). Not surprisingly, at 2 days after NMDA treatment the levels of pS6 were potently inhibited by rapamycin (Fig. 4F,G), whereas levels of cFos, p38 MAPK, Egr1 and pCREB (not shown) were unaffected. The effects of rapamycin on the proliferation of MGPCs and levels of pS6 were dose dependent (Fig. 4D-H). There was a correlation between the levels of pS6 and the number of proliferating MGPCs (Fig. 4F). Indeed, the vast majority (88.5±6.1%; n=5) of EdU-labeled, proliferating MGPCs were positive for pS6 (Fig. 4I). However, many (48.8±13.2%; n=5) Müller glia were positive for pS6 but negative for EdU (Fig. 4L), suggesting that activation of mTor might not be sufficient to drive cells back into the cell cycle.

We tested whether the de-differentiation of Müller glia was affected by mTor inhibition by assaying for the stem cell factors Pax6 and Klf4. Pax6 and Klf4 are not normally expressed by Müller glia, but are upregulated in response to stimuli that promote the reprogramming of Müller glia into MGPCs (Todd and Fischer, 2015). Inhibition of mTor with rapamycin had no effect upon the upregulation of Pax6 and Klf4 in Müller glia at 2 days after NMDA treatment (Fig. 4J,K), suggesting that the de-differentiation of Müller glia was not blocked by inhibition of mTor and that upregulation of Pax6 and Klf4 is not sufficient to drive proliferation. To test whether mTor signaling is downstream of MAPK in damaged retinas, we applied the MEK inhibitor UO126 following NMDA treatment and assayed for proliferation and levels of pS6. Consistent with previous reports (Fischer et al., 2009b), UO126 significantly inhibited the proliferation of MGPCs (Fig. 4L,M). However, inhibition of MEK with UO126 failed to influence the levels of pS6 in Müller glia/MGPCs (Fig. 4N,O). These findings suggest that activation of mTor is not sufficient to drive the proliferation of MGPCs, and that the activation of mTor does not require MAPK signaling in damaged retinas.

The inhibition of mTor in damaged retinas might delay, rather than block, the proliferation of MGPCs. Accordingly, we assayed for the formation of proliferating MGPCs 3 days after NMDA treatment. Rapamycin potently inhibited the accumulation of BrdU in MGPCs in central and peripheral regions of damaged retinas (Fig. 5A,B). In addition, rapamycin inhibited the proliferation of microglia and NIRG cells (Fig. 5A,B), which are known to proliferate in damaged retinas (Zelinka et al., 2012). To confirm the findings of BrdU-incorporation studies, we assayed for levels of phospho-histone H3 (pHisH3) to identify cells in late G2 and M-phase of the cell cycle. Consistent with the BrdU labeling studies, we found that rapamycin significantly reduced the numbers of pHisH3-positive cells in the retina (Fig. 5C,D). MGPCs are known to transiently express pHisH3 and neurofilament during reprogramming into proliferating progenitor cells (Fischer et al., 2004; Fischer and Reh, 2001). Thus, we tested whether inhibition of mTor influenced the expression of neurofilament in MGPCs. We found a significant decrease in the number of neurofilament-positive MGPCs in damaged retinas treated with rapamycin (Fig. 5E,F). All (n=148 cells) of the neurofilament-expressing MGPCs were positive for pHisH3 and had a cytoplasmic distribution of Sox2 (Fig. 5G). These observations are consistent with the hypotheses that MGPCs in M-phase are positive for

Development (2016) 143, 1859-1873 doi:10.1242/dev.133215

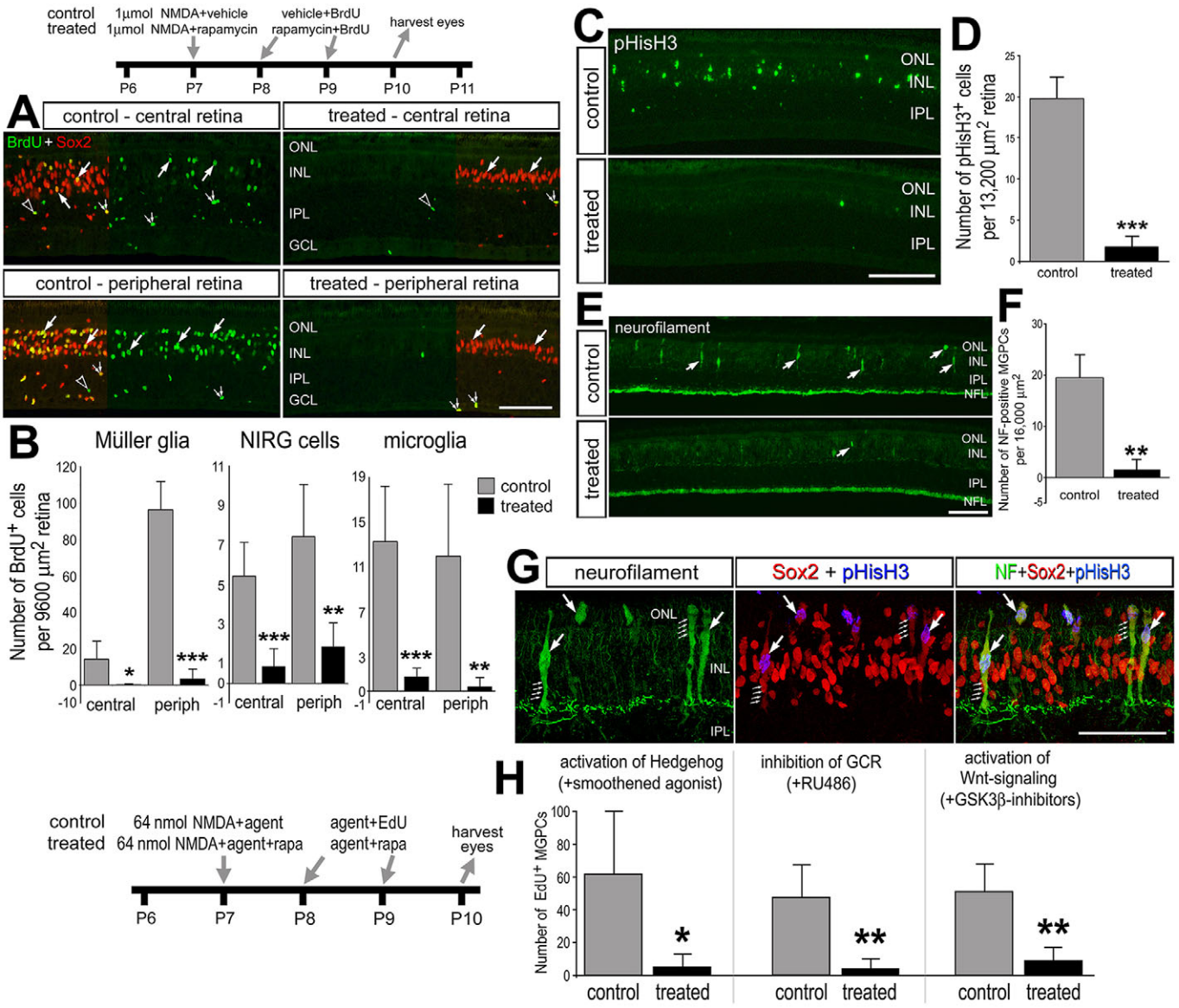

Fig. 5. Rapamycin inhibits the formation of proliferating MGPCs in damaged retinas. (A-G) Eyes were injected with a high dose (1 μmol) of NMDA± rapamycin at P7, vehicle+BrdU or rapamycin+BrdU at P8 and P9, and retinas harvested at P10. (H) Eyes were injected with a low dose (64 nmol) NMDA+SAG or RU486 or GSK3β inhibitors±rapamycin at P7, SAG or RU486 or GSK3β inhibitors+BrdU±rapamycin at P8 and P9, and retinas harvested at P10. Sections of the retina were labeled with antibodies to Sox2, BrdU (A), pHisH3 (C), neurofilament (E) and neurofilament, Sox2 and pHisH3 (G). (A) Sox2 is included as a partial field overlay to indicate the nuclei of Müller glia and NIRG cells. Images and cell counts were made from central (A,B) and peripheral (A-H) regions of retina. Bar charts illustrate the mean (±s.d.; $n \geq 6$) number of (B) proliferating BrdU-labeled Müller glia/MGPCs, NIRG cells and microglia, (D) pHisH3$^+$ MGPCs, (F) neurofilament$^+$ MGPCs, and (H) BrdU-labeled MGPCs. *P<0.05, **P<0.001, ***P<0.0001, unpaired, two-tailed t-test. Arrows indicate nuclei of Müller glia/MGPCs labeled for BrdU; small double-arrows indicate NIRG cells labeled for BrdU; open arrowheads indicate microglia labeled for BrdU; and four consecutive small arrows indicate the processes of MGPCs labeled for neurofilament and Sox2 (cells in M-phase where the nuclear envelope has dissolved). Scale bars: 50 μm.

pHisH3 and lack a nuclear envelope, which would otherwise restrict the subcellular distribution of transcription factors, and that rapamycin potently suppresses the formation of MGPCs. Similar to the effects of rapamycin, the mTor inhibitor ridaforolimus inhibited the formation of proliferating MGPCs in damaged retinas (Fig. S1C-E).

The formation of MGPCs can be stimulated in retinas that have sustained low levels of damage by activating Hedgehog (Todd and Fischer, 2015) or Wnt (Gallina et al., 2016) signaling or inhibiting glucocorticoid signaling (Gallina et al., 2014b). Accordingly, we tested whether inhibition of mTor overrides the actions of Hedgehog, glucocorticoid and Wnt signaling on increasing the proliferating MGPCs in modestly damaged retinas. Inhibition of mTor potently suppressed the proliferation of MGPCs in damaged retinas treated with Hedgehog agonist, glucocorticoid receptor antagonist, or a cocktail of GSK3β inhibitors (Fig. 5H).

To better understand how inhibition of mTor might impact the formation of MGPCs, we assayed for Pax6 expression and accumulation of nuclear β-catenin. In different models of retinal regeneration, Pax6 expression and Wnt signaling (accumulation of nuclear β-catenin) are known to be important for the formation of MGPCs (Gallina et al., 2016; Osakada et al., 2007; Ramachandran et al., 2011; Thummel et al., 2010). We found that levels of Pax6 are not significantly affected in Müller glia/MGPCs treated with

Development (2016) 143, 1859-1873 doi:10.1242/dev.133215

rapamycin (Fig. 6A), when standardizing levels to account for rapamycin-mediated decreases in cell number across cells in the ONL and INL (not shown). However, there were fewer Pax6/Sox9-positive cells in the ONL of rapamycin-treated retinas (Fig. 6A,B). Nuclear migration may be required for the reprogramming of Müller glia to a more progenitor-like state (Lahne et al., 2015). We found

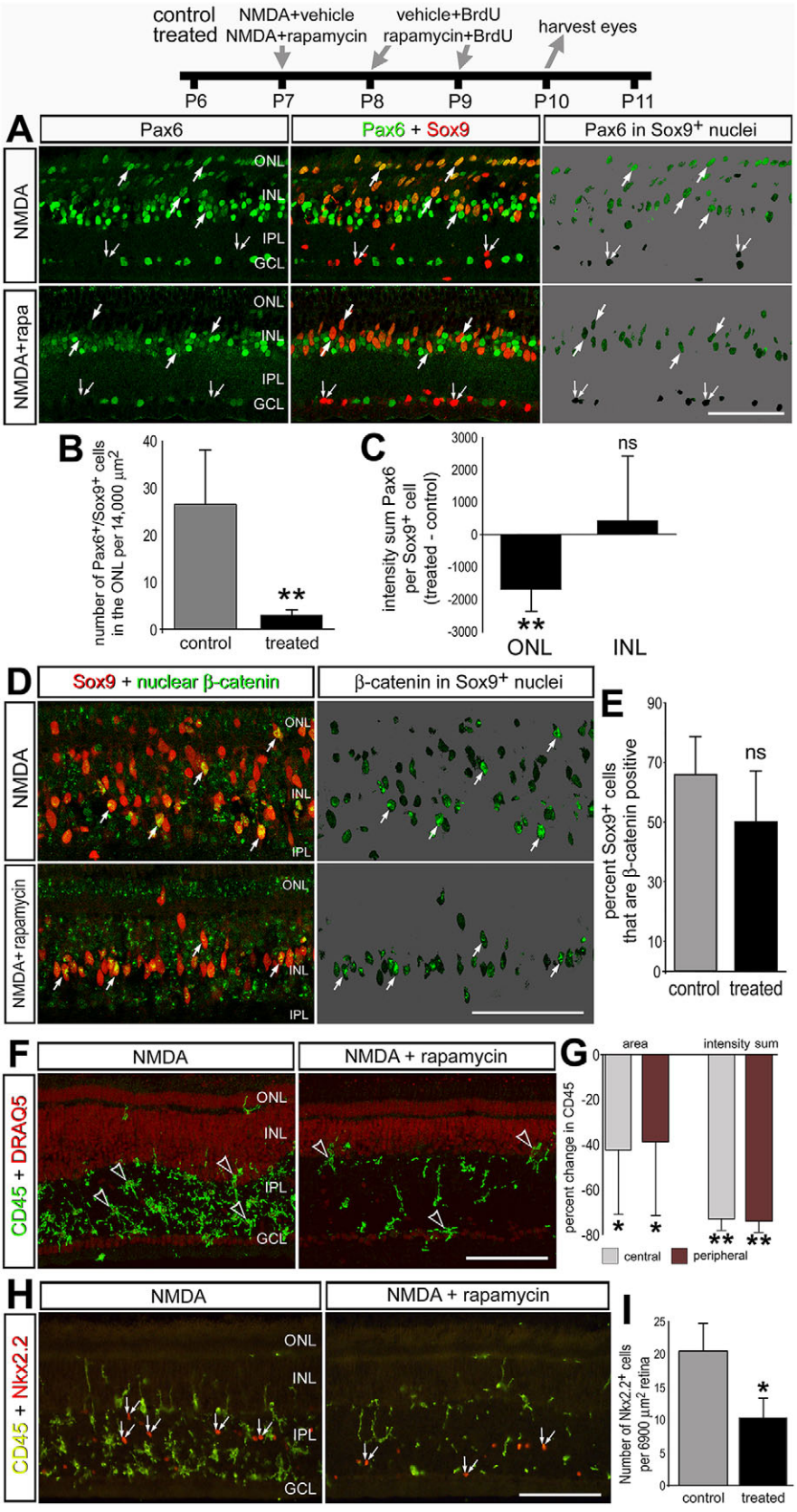

Fig. 6. Inhibition of mTor in NMDA-damaged retinas suppresses the nuclear migration and Pax6 expression in MGPCs, and suppresses the accumulation of microglia and NIRG cells. Rapamycin inhibits neurofilament expression in MGPCs and inhibits the accumulation of reactive microglia and NIRG cells in NMDA-damaged retinas. Eyes were injected with NMDA±rapamycin at P7, vehicle+BrdU or rapamycin+BrdU at P8 and P9, and retinas harvested at P10. Sections of the retina were labeled with antibodies to Pax6 and Sox9 (A), nuclear β-catenin and Sox9 (D), CD45 (F) or Nkx2.2 and CD45 (H). DRAQ5 was used to label nuclei in F. (B) The mean (±s.d.; n=5) number of Pax6$^+$/Sox9$^+$ cells in the ONL. (C) The mean (treated – control; ±s.d.; n=5) intensity sum of Pax6 immunofluorescence per Sox9$^+$ nucleus in the ONL or INL. (E) The mean (±s.d.; n=5) percentage change in the area of pixels above threshold, and the percentage change in the sum of pixel values above threshold. (G) The mean (±s.d.; n=8) number of NIRG cells in control and treated retinas. *P<0.05, **P<0.005 by (B,E,I) unpaired, two-tailed t-test or (C,G) Mann–Whitney U-test. Arrows indicate the nuclei of Müller glia/MGPCs; small double-arrows indicate NIRG cells; and open arrowheads indicated microglia. Scale bars: 50 µm.

Development (2016) 143, 1859-1873 doi:10.1242/dev.133215

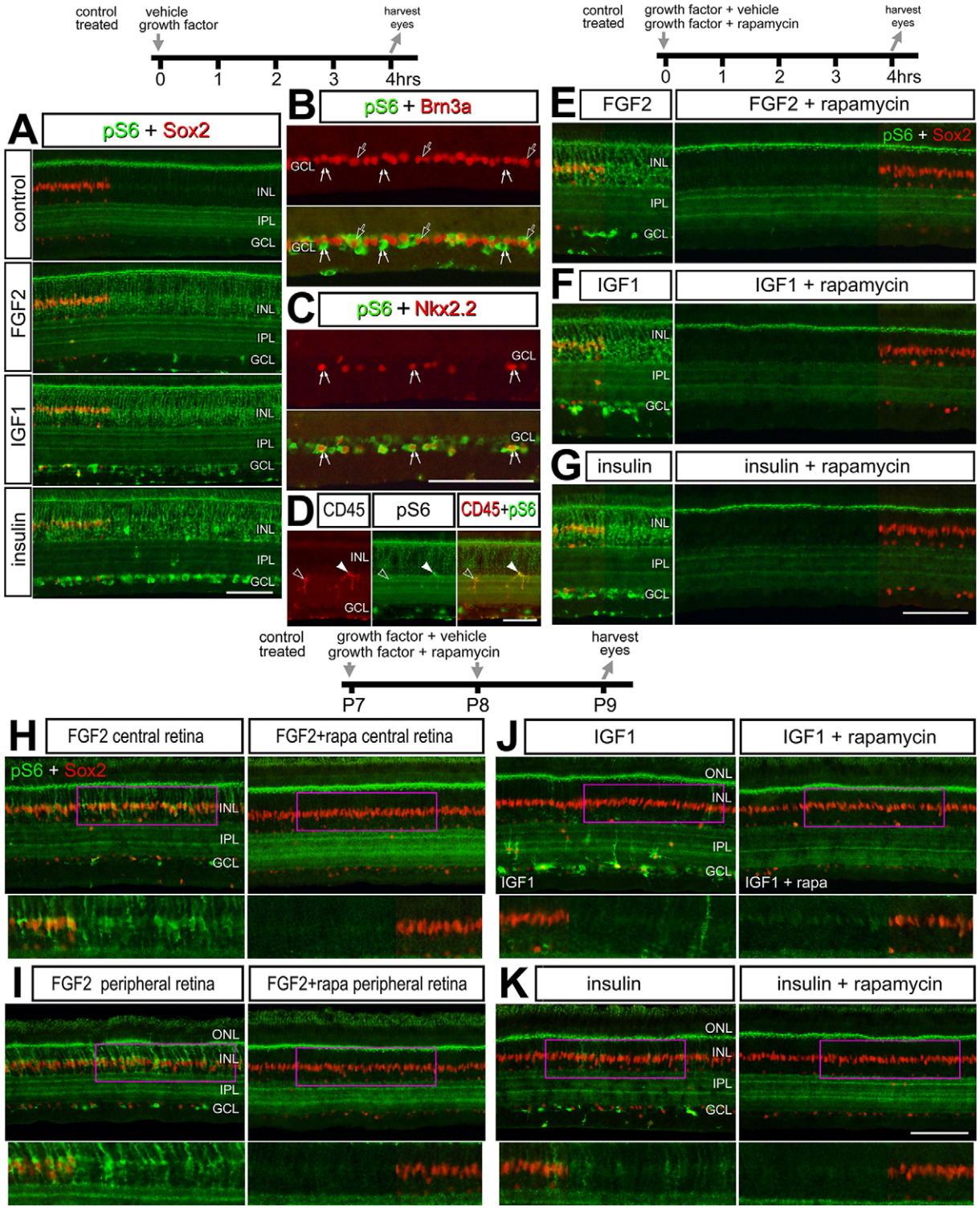

Fig. 7. pS6 accumulation is robustly induced in Müller glia and inner retinal cells by FGF2, IGF1 and insulin, and this induction is blocked by rapamycin. Retinas were obtained from eyes that were injected with growth factor or vehicle and harvested 4 h later (A-D), injected with growth factor±rapamycin and harvested 4 h later (E-G), or growth factor±rapamycin at P7 and P8, and harvested at P9 (H-K). Retinal sections were labeled with antibodies to pS6 and Sox2 (A-D,H-K), Brn3a (B), Nkx2.2 (C) or CD45 (D). Sox2 is included as a partial field overlay to indicate the nuclei of Müller glia (A,E-K). (H-K) Boxed regions are enlarged (2×) beneath. Open arrows indicate $Brn3a^{+}/pS6^{+}$ ganglion cells; small double-arrows indicate $pS6^{+}$ NIRG cells; open arrowheads indicate $pS6^{-}$ microglia; and solid arrowheads indicate $pS6^{+}$ microglia. Scale bars: 50 µm (in A for A; in C for B,C; in G for E-G; in K for H-K).

significantly lower levels of Pax6/cell in the few Sox9-positive glia that migrated into the ONL in rapamycin-treated retinas compared with controls, whereas levels of Pax6 in the Sox9-positive glia that were in the INL were not significantly different from controls (Fig. 6C). The percentage of Sox9-positive Müller glia/MGPCs that were positive for nuclear β-catenin was not significantly affected by

Development (2016) 143, 1859-1873 doi:10.1242/dev.133215

treatment with rapamycin (Fig. 6D,E). These findings suggest that the inhibition of mTor and associated decreases in proliferation of MGPCs do not result from decreases in Wnt/β-catenin signaling.

Reactive microglia and/or NIRG cells are known to promote the formation of proliferating MGPCs in damaged and FGF2-treated retinas (Fischer et al., 2014). Accordingly, we examined whether inhibition of mTor influenced the microglia and NIRG cells in damaged retinas. Rapamycin had a significant effect upon the reactivity and accumulation of microglia/macrophages and NIRG cells in damaged retinas. The abundance of CD45-positive microglia/macrophages and Nkx2.2-positive NIRG cells was reduced by rapamycin in NMDA-damaged retinas (Fig. 6F-I).

mTor signaling is activated in response to insulin, IGF1 and FGF2

FGF2/MAPK signaling stimulates Müller glia to give rise to progenitor cells (Fischer et al., 2009a,b) and is sufficient to stimulate the formation of proliferating MGPCs in the absence of damage (Fischer et al., 2014). Further, in combination, insulin/IGF1 and FGF2 act synergistically to stimulate the formation of MGPCs in chick and zebrafish retinas (Ritchey et al., 2012; Wan et al., 2014). We tested whether a single injection of FGF2, IGF1 or insulin activates mTor signaling. FGF2, IGF1 and insulin stimulated the accumulation of pS6 in Müller glia (Fig. 7A). In addition, pS6 was observed in a few scattered cells in the GCL and IPL in response to FGF2. These cells were more abundant in retinas treated with IGF1, and even more prevalent in retinas treated with insulin (Fig. 7A-C). In insulin-treated retinas, the pS6-accumulating cells included Brn3a-positive ganglion cells (Fig. 7B), Nkx2.2-positive NIRG cells or oligodendrocytes (Fig. 7C), and CD45-positive microglia (Fig. 7D). Rapamycin completely inhibited the accumulation of pS6 that was rapidly induced by treatment with FGF2, IGF1 or insulin (Fig. 7E,F). Similar to the effects of rapamycin, ridaforolimus inhibited the upregulation of pS6 4 h after FGF2 treatment (Fig. S1F,G).

We examined how sustained treatment with growth factors influences mTor signaling, since sustained exposure to FGF2 with or without insulin/IGF1 stimulates the formation of MGPCs (Fischer et al., 2002, 2014). Two consecutive daily injections of FGF2 resulted in persistent pS6 in Müller glia, and the levels of pS6 appeared elevated in peripheral regions compared with central regions of the retina (Fig. 7H,I). By comparison, two consecutive daily injections of IGF1 or insulin resulted in persistent pS6 immunoreactivity in glia-like cells scattered across inner layers of the retina, but not in Müller glia (Fig. 7J,K). Rapamycin completely blocked the accumulation of pS6 in all cell types that resulted from long-term treatment with FGF2, IGF1 or insulin (Fig. 7H-K).

mTor signaling and the formation of MGPCs in FGF2-treated retinas

Four consecutive daily intraocular injections of FGF2 are sufficient to stimulate the formation of proliferating MGPCs in the absence of retinal damage (Fischer et al., 2014). We tested whether inhibition of mTor influences the formation of MGPCs in FGF2-treated retinas. Addition of rapamycin with the last two doses of FGF2 potently suppressed the proliferation of MGPCs in peripheral regions of the retina (Fig. 8A,B). Although the proliferation of MGPCs was suppressed by rapamycin, the nuclear migration of Müller glia remained widespread (Fig. 8A, B). In addition, rapamycin inhibited the proliferation of NIRG cells and microglia in FGF2-treated retinas (Fig. 8B). Consistent with the notion that rapamycin inhibits mTor signaling in FGF2-treated retinas, levels of pS6 in the Müller glia/MGPCs were suppressed 24 h after the last injection (Fig. 8C). By comparison, MAPK signaling was not impaired in Müller glia treated with FGF2 and rapamycin, as compared with readouts of MAPK signaling seen in Müller glia treated with FGF2 alone. Inhibition of mTor had no effects upon levels of pERK1/2 (Fig. 8D), p38 MAPK, pCREB, cFos or Egr1 (not shown) in FGF2-treated Müller glia. Unlike Müller glia treated with rapamycin in NMDA-damaged retinas, Pax6 was nearly absent whereas levels of Klf4 remained elevated in Müller glia treated with FGF2 and rapamycin, as compared with levels seen in Müller glia treated with FGF2 alone (Fig. 8E,F). Similar to the effects of rapamycin, ridaforolimus suppressed the proliferation of MGPCs in FGF2-treated retinas (Fig. S1H-J).

FGF2 treatment is known to increase expression of *Notch1*, *Hes5*, *Ascl1a*, *c-Myc*, *C3aR* and *C3*, and these increases can be blocked by glucocorticoid signaling (Gallina et al., 2014b). Increased levels of *Notch1*, *Hes5*, *Ascl1a* and *c-Myc* have been associated with phenotypic transitions between Müller glia and progenitor cells (Gallina et al., 2014a; Ghai et al., 2010; Hayes et al., 2007; Nelson et al., 2011), and complement C3a peptide and C3a receptor (C3aR) are involved in the regeneration of embryonic retina (Haynes et al., 2013). We found that application of rapamycin with FGF2 had no effect on the expression levels of *Notch1*, *Hes5*, *Ascl1a*, *c-Myc* and *C3*, whereas levels of *C3aR* were further increased (Fig. 8G). These findings suggest that the reprogramming-associated actions of *Notch1*, *Hes5*, *Ascl1a* and *c-Myc* are not affected by mTor signaling, whereas increased levels of *C3aR* might be downstream of inhibited mTor signaling in Müller glia/MGPCs. Levels of *C3* and *C3aR* tend to be downregulated when the formation of MGPCs is suppressed by activation of glucocorticoid signaling (Gallina et al., 2014b), inhibition of Hedgehog signaling (Todd and Fischer, 2015) or the ablation of microglia (Fischer et al., 2014).

DISCUSSION

Our findings suggest that mTor signaling is required for the formation of proliferating MGPCs in retinas damaged by NMDA or treated with FGF2 in the absence of damage. Inhibition of mTor with rapamycin potently and selectively suppressed signaling, decreasing levels of pS6 in Müller glia/MGPCs as well as microglia and NIRG cells. We find that a PTEN inhibitor, IGF1 and insulin activate mTor signaling in Müller glia, but this is not sufficient to drive the formation of MGPCs. By comparison, activation of mTor signaling by FGF2 appears to result in sustained activation of signaling, and repeated treatment with FGF2 is sufficient to stimulate the formation of proliferating MGPCs (Fischer et al., 2014). Further, inhibition of mTor effectively blocks the effects of sustained exposure to FGF2 on the reprogramming of Müller glia to proliferating MGPCs.

In developing retinas, mTor signaling is active in immature neurons and glia at different stages of development. We find pS6 in scattered immature ganglion cells, amacrine cells and Müller glia. These findings suggest context- and cell type-specific roles for mTor signaling during retinal development. mTor signaling may be transiently activated during the maturation of retinal cells and, therefore, appears in scattered ganglion, amacrine or Müller cells. By comparison, levels of pS6 in normal, mature retina are very low or absent in neurons and glia. However, there is a significant accumulation of pS6 in glia following NMDA-induced damage or FGF2 treatment in the absence of damage. Following NMDA

Development (2016) 143, 1859-1873 doi:10.1242/dev.133215

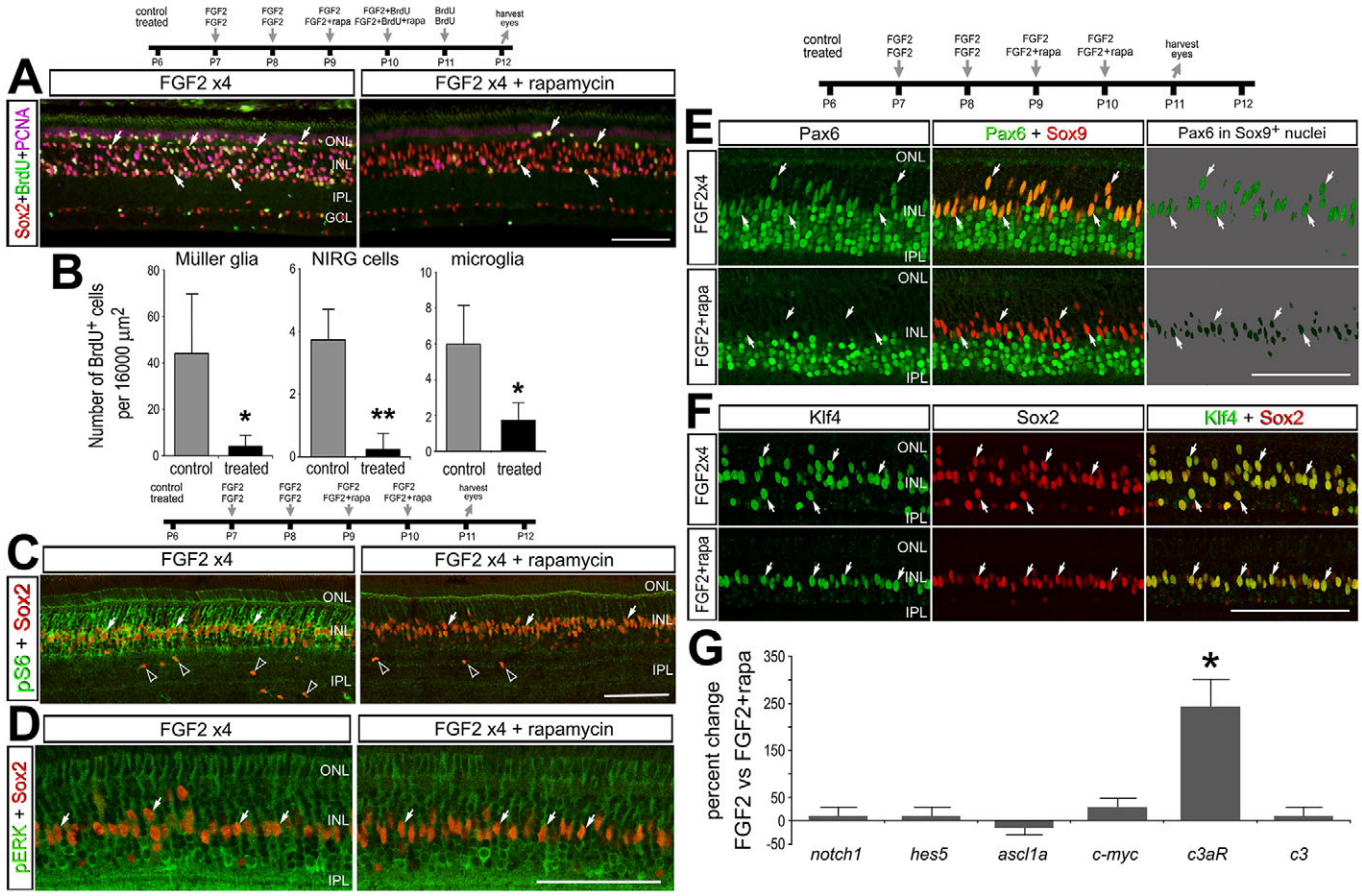

Fig. 8. Rapamycin inhibits the formation of proliferating MGPCs in FGF2-treated retinas in the absence of damage. Retinas were obtained from eyes that were injected with FGF2 at P7 and P8, FGF2±rapamycin at P9, FGF2 and BrdU±rapamycin at P10, BrdU at P11, and harvested at P12 (A-D), or harvested at P11 without the injection of BrdU (E-G). Retinal sections were labeled with antibodies to BrdU, PCNA and Sox2 (A), pS6 and Sox2 (C), pERK1/2 and Sox2 (D), Pax6 and Sox9 (E) or Klf4 and Sox2 (F). (B) The mean (±s.d.; n=6) number of proliferating Müller glia, NIRG cells and microglia in peripheral regions of control and treated retinas. *P<0.05, **P<0.001, unpaired, two-tailed t-test. (G) qRT-PCR was used to measure retinal levels of *Notch1*, *Hes5*, *Ascl1a*, *c-Myc*, *C3aR* and *C3*. *P<0.05 (n=4), two-tailed Mann–Whitney U-test. Scale bars: 50 µm.

treatment, pS6 expression peaks at 4 h, suggesting that the mTor signaling is rapidly activated in Müller glia after damage to retinal neurons. Inhibition of PTEN in normal retina resulted in a rapid transient upregulation of pS6 in Müller glia. This finding suggests that signaling through PI3K/Akt might be present in Müller glia under normal conditions, but the pathway is kept quiescent by PTEN. However, in NMDA-damaged retinas, inhibition of PTEN failed to stimulate the formation of proliferating MGPCs, and inhibition of PI3K or Akt failed to suppress the formation of proliferating MGPCs. It is expected that inhibition of PTEN should increase signaling through Akt and mTor to increase retinal levels of pS6 in damaged retinas. Further, inhibition of PTEN failed to increase the levels of pS6 at 3 days after NMDA treatment (not shown). These findings suggest that signaling through PI3K/Akt might not contribute to the reprogramming of Müller glia into proliferating MGPCs in damaged chick retina (Fig. 9). By contrast, PI3K/Akt signaling is an important ‘hub’ in the network of pathways required for the formation of MGPCs in the zebrafish retina (Wan et al., 2014). During development of the mammalian retina, loss of function of PTEN, leading to gains in PI3K/Akt signaling, disrupts the mosaic patterning and dendritic morphogenesis of inner retinal neurons, whereas cell proliferation and cell fate are unaffected (Sakagami et al., 2012; Cantrup et al., 2012). Collectively, these findings indicate context- and species-specific functions of PI3K/Akt and mTor signaling in developing and regenerating retina.

Cross-talk between FGF/MAPK signaling and mTor is required for the formation of proliferating MGPCs (Fig. 9). It has been shown that there is cross-talk between FGF2/MAPK and mTor/S6K2 in regulating the proliferation of small cell lung cancer cell lines (De Luca et al., 2012; Pardo et al., 2001; Ma et al., 2005). pERK1/2 is known to inhibit TSC1/2, thereby relieving inhibition of RHEB to active mTORC1 (Ciuffreda et al., 2014). In the developing eye, thrombin-induced proliferation of RPE cells is driven by ERK-dependent activation of mTORC1 (Parrales et al., 2013). We found that inhibition of PI3K with LY294002 had no effect on the formation of MGPCs in damaged chick retina (Fig. 9). By contrast, in the zebrafish model it has been shown that inhibition of PI3K with LY294002 potently inhibits the formation of proliferating MGPCs in response to retinal damage (Paliouras et al., 2012). EGF signaling through mTor is known to regulate the transit-amplifying progenitor cells isolated from adult forebrain (Paliouras et al., 2012). In the chick model, we found that inhibition of PI3K or Akt failed to influence the accumulation of pS6 and also failed to influence the proliferation of MGPCs in NMDA-damaged retinas, unlike the inhibition of mTor, which suppresses both the accumulation of pS6 and the proliferation of MGPCs (Fig. 9). Similarly, inhibition of FGF receptors or MAPK signaling suppresses the proliferation of

Development (2016) 143, 1859-1873 doi:10.1242/dev.133215

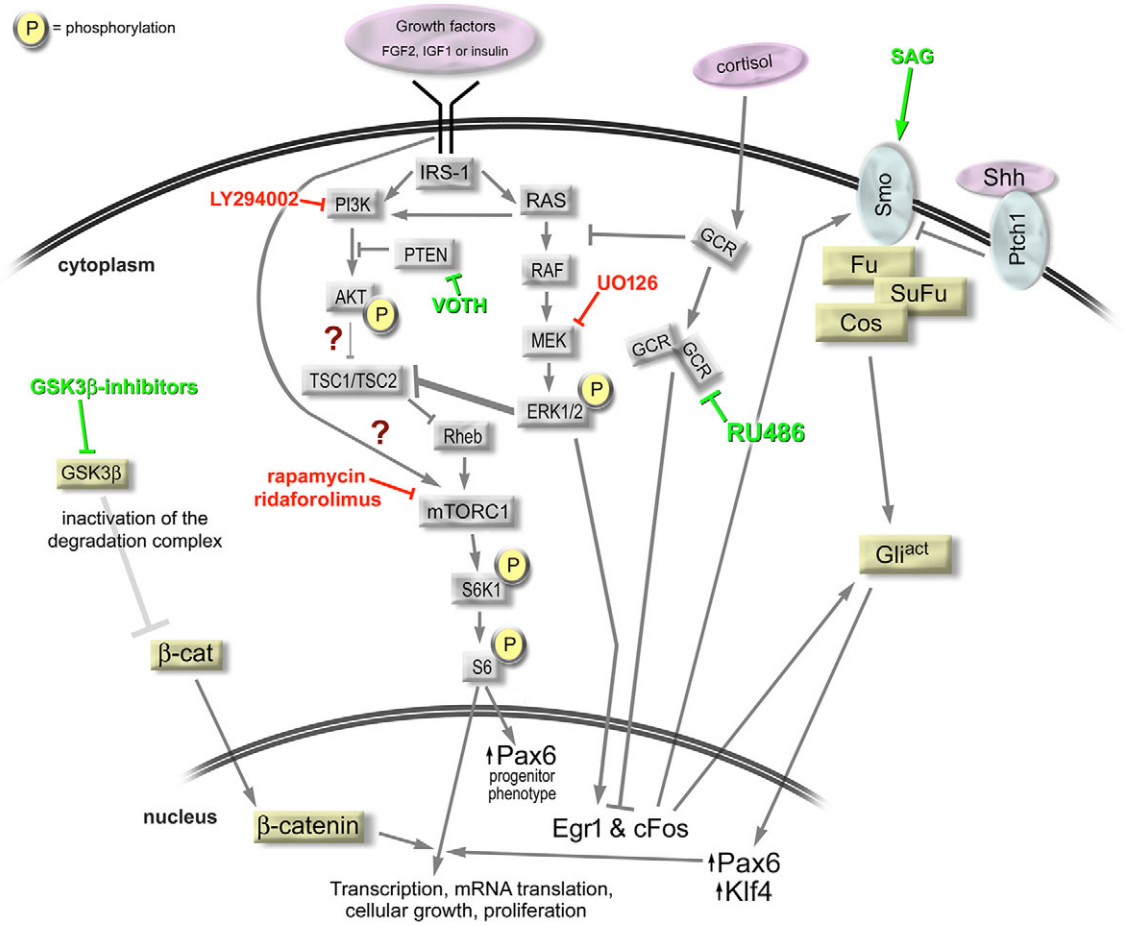

Fig. 9. Summary of the cell signaling pathways and inhibitors that influence the formation of proliferating MGPCs. Green text and lines indicate activators and red text and lines indicate inhibitors of MGPC formation. The schematic incorporates recent findings regarding the roles of Wnt/β-catenin and Hedgehog signaling in stimulating the formation of MGPCs (Fischer et al., 2010; Gallina et al., 2016) and current findings that these signaling pathways require mTor signaling for the formation of proliferating MGPCs. Our findings suggest that signaling through pERK is key to activating mTor, whereas signaling through PI3K and Akt might not activate mTor during the formation of MGPCs.

MGPCs in damaged retinas (Fischer et al., 2009b; Wan et al., 2014), whereas inhibition of MAPK does not suppress the activation of mTor (current study). Collectively, these findings suggest that activation of mTor in Müller glia/MGPCs may occur independently of PI3K/Akt and MAPK signaling in damaged retinas, where many different pathways are in play (Fig. 9). We found that inhibition of mTor had no effect on the MAPK pathway, whereas pS6 accumulation and proliferation of MGPCs were potently blocked by inhibition of mTor in FGF2-treated retinas. However, activation of mTor can also phosphorylate 4EBP1 (EIF4EBP1) to relieve inhibition of eIF4E to initiate the translation of proteins (reviewed by Sawyers, 2008; Dazert and Hall, 2011). We cannot exclude the possibility that mTor signaling through 4EBP1 and eIF4E, in addition to signaling through p70S6K and pS6, might be involved in the formation of proliferating MGPCs.

A network of cell signaling pathways is known to be activated during the reprogramming of Müller glia into proliferating MGPCs in both the zebrafish and chick model systems (Gallina et al., 2016; Todd and Fischer, 2015; Wan et al., 2014). In zebrafish, MAPK and PI3K signaling converge and 'bottleneck' through Jak/Stat and β-catenin signaling (reviewed by Gallina et al., 2014a). In the chick, we provide evidence that MAPK, Hedgehog, glucocorticoid and Wnt/β-catenin signaling converge and require mTor signaling (Fig. 9). As a notable difference from zebrafish (Wan et al., 2014), our findings suggest that signaling through PI3K and Akt does not have a significant impact on the formation of chick MGPCs. We provide evidence that inhibition of mTor overrides the MGPC-promoting effects of activating Hedgehog and Wnt/GSK3β signaling, and of inhibiting glucocorticoid receptor (GCR) signaling. Wnt signaling (nuclear β-catenin), MAPK signaling (pERK) and Klf4 remain high in MGPCs in retinas treated with mTor inhibitor, whereas levels of Pax6 are suppressed, more noticeably in FGF2-treated retinas. These findings suggest that mTor signaling is downstream of Klf4, Wnt signaling and FGF2/MAPK signaling, and that upregulation of Pax6 is downstream of mTor signaling, particularly in undamaged retina (Fig. 9). Activation of GCR signaling is known to antagonize FGF2/MAPK signaling, and inhibition of GCR stimulates the formation of proliferating MGPCs (Wan et al., 2014). Thus, mTor signaling may be potentiated downstream of inhibition of GCR. Nevertheless, GCR antagonist failed to promote the formation of MGPCs in damaged retinas treated with mTor inhibitor. Collectively, these findings suggest that the network of signaling pathways that are activated during the formation of MGPCs requires activation of mTor.

We found different patterns of pS6 accumulation in response to intraocular injections of insulin, IGF1 and FGF2. In addition, we found persistent pS6 in Müller glia 24 h after treatment with FGF2,

Development (2016) 143, 1859-1873 doi:10.1242/dev.133215

whereas treatment with IGF1 or insulin resulted in persistent pS6 accumulation in presumptive microglia and/or NIRG cells. This is consistent with findings that IGF1 and insulin stimulate the reactivity and proliferation of microglia and NIRG cells (Fischer et al., 2010; Gallina et al., 2014a). The pattern and temporal dynamics of pS6 accumulation that result from intraocular injections of FGF2, insulin and IGF1 are likely to result from different patterns of receptor expression and components of cell signaling. Our findings indicate that activation of mTor and increased levels of pS6 are not sufficient to induce the formation of proliferating MGPCs. In addition, ridaforolimus effectively blocked the upregulation of pS6 in both NMDA-damaged and FGF2-treated retinas, but this inhibitor was not as effective as rapamycin in suppressing the proliferation of MGPCs (see Fig. S1); this probably resulted from different pharmacodynamics. Thus, it is likely that the duration of mTor activation and the pharmacodynamics of the inhibitor are relevant to the formation of proliferating MGPCs.

Conclusions

The mTor pathway is active in late-stage progenitors, differentiating neurons and glia in the developing retina. The mTor pathway is transiently activated in Müller glia undergoing de-differentiation into proliferating MGPCs and in response to growth factors including insulin, IGF1 and FGF2. Inhibition of mTor prevents the proliferation of MGPCs in both damaged and FGF2-treated retinas, whereas inhibition of PI3K had no effect. Inhibition of PTEN activates mTor signaling in normal retina, but has no effect on the formation of MGPCs in damaged retina. Although inhibition of MAPK signaling suppresses the proliferation of MGPCs, mTor signaling remains unimpaired. Signaling through mTor is required for the MGPC-promoting effects of activation of Wnt/β-catenin and Hedgehog signaling or of inhibition of GCR signaling in damaged retinas. We conclude that the activation of mTor by NMDA-mediated damage or by growth factors is necessary, but not sufficient, for the formation of MGPCs.

MATERIALS AND METHODS

Animals

The use of animals in these experiments was in accordance with guidelines established by the National Institutes of Health and the Ohio State University. This study was approved by the Institutional Animal Care and Use Committee (IACUC). Fertilized eggs were obtained from Meyer Hatchery (Polk, Ohio). Eggs were incubated between 36.6°C and 37.8°C and embryos were staged according to guidelines set by Hamburger and Hamilton (1951). Newly hatched leghorn chickens (*Gallus gallus domesticus*) were obtained from Meyer Hatchery and kept on a 12/12 h light/dark cycle (lights on at 07:00 am). Chicks were housed in a brooder at ~25°C and received water and Purina chick starter *ad libitum*.

Intraocular injections

Chickens were anesthetized and eyes injected as described previously (Fischer et al., 1998a,b). One dose represents the single delivery of a compound into the vitreous chamber of the eye. The dose (µg or ng) of each compound is provided with an estimated initial maximum concentration at the retina assuming a volume of liquid vitreous of 200 µl. Compounds used in these studies included the PTEN inhibitor VO-OHpic trihydrate (VOTH; 500 ng to 1 µg/dose, or 6.0 µM to 12.0 µM; Sigma-Aldrich), PI3K inhibitor LY294002 (1 µg/dose or 16.3 µM; Sigma-Aldrich), mTor inhibitor ridaforolimus (1 µg/dose or 0.29, 1.15 and 4.9 µM; Sigma-Aldrich), mTor inhibitor rapamycin (0.063, 0.25 and 1 µg/dose, or 0.29, 1.15 and 4.6 µM; Sigma-Aldrich), smoothened agonist (SAG; 500 ng/dose or 4.2 µM; EMD Millipore), glucocorticoid receptor inhibitor RU486 (1 µg/dose or 11.6 µM; Sigma-Aldrich), a cocktail of three different GSK3β inhibitors that included 1-azakenpaullone (500 ng/dose or 7.6 µM; Selleck Chemicals), BIO (500 ng/dose or 7.0 µM; R&D Systems) and CHIR 99021 (500 ng/dose or 5.4 µM; R&D Systems), FGF2 (200 ng/dose or 46 nM; Sigma-Aldrich), UO126 (800 ng/dose or 2.4 µM; Sigma-Aldrich) and NMDA (38.5 or 154 µg/dose, 5 mM or 20 mM; Sigma-Aldrich). 1 µg BrdU or EdU was injected to label proliferating cells. Injection paradigms are included in the figures. Vehicle was 30% DMSO in saline for the injections of all small-molecule inhibitors.

Tissue dissection, fixation, sectioning and immunolabeling

Tissues were fixed, sectioned and immunolabeled as described previously (Fischer et al., 1998a; Ghai et al., 2008; Stanke et al., 2010). Working dilutions and sources of antibodies are listed in Table S1. Secondary antibodies included donkey anti-goat Alexa 488/568, goat anti-rabbit Alexa 488/568/647, goat anti-mouse Alexa 488/568/647 and goat anti-rat Alexa 488 (Invitrogen) diluted 1:1000 in PBS plus 0.2% Triton X-100. DRAQ5 (Biostatus) was diluted to 5 µM in the secondary antibody solution to fluorescently stain nuclear DNA.

Labeling for EdU

Immunolabeled sections were fixed in 4% formaldehyde in PBS for 5 min at room temperature, washed for 5 min with PBS, permeabilized with 0.5% Triton X-100 in PBS for 1 min at room temperature, and washed twice for 5 min each in PBS. Sections were incubated for 30 min at room temperature in 2 M Tris pH 8.5, 50 mM $CuSO_4$, Alexa Fluor 568 azide (Thermo Fisher Scientific) and 0.5 M ascorbic acid in distilled water. Sections were washed with PBS for 5 min and further processed for immunofluorescence as required.

Quantitative PCR

cDNA was synthesized as described using standard protocols and qRT-PCR performed as described previously (Fischer et al., 2004, 2010; Zelinka et al., 2012). PCR primers were designed using the Primer-BLAST design tool at NCBI (http://www.ncbi.nlm.nih.gov/tools/primer-blast/). Forward and reverse primer sequences (5′-3′) and predicted product sizes are listed in Table S2. Ct values obtained from real-time PCR were normalized to *Gapdh* and the fold difference between control and treated samples was determined using the ΔΔCt method and represented as a percentage change from control values. PCR reactions were performed using standard protocols, SYBR Green Master Mix (Life Technologies) and an Applied Biosystems StepOne Plus thermal cycler.

Terminal deoxynucleotidyl transferase dUTP nick end labeling (TUNEL)

To identify dying cells that contained fragmented DNA the TUNEL method was used. We used an *In Situ* Cell Death Kit (TMR Red; Roche Applied Science) as per the manufacturer's instructions.

Microscopy, quantitative immunofluorescence and cell counts

Wide-field photomicrographs were obtained using a Leica DM5000B microscope and Leica DC500 digital camera. Confocal images were obtained with a Zeiss LSM510 at the Hunt-Curtis Imaging Facility in the Department of Neuroscience, Ohio State University. Images were optimized for color, brightness and contrast, multiple-channel images overlaid, and figures constructed using Adobe Photoshop 6.0. Cell counts were made from at least five different animals, and means and standard deviations calculated on data sets. To avoid the possibility of region-specific differences within the retina, cell counts were consistently made from the same region of retina for each data set. Central retina was defined as the region within a 3 mm radius of the posterior pole of the eye, and peripheral retina was defined as an annular region between 3 mm and 0.5 mm from the ciliary marginal zone.

Similar to previous reports (Fischer et al., 2009b, 2010; Ghai et al., 2009), immunofluorescence was quantified using ImagePro 6.2 (Media Cybernetics). Identical illumination, microscope, and camera settings were used to obtain images for quantification. Retinal areas were sampled from digital images. Areas were sampled over the INL and outer nuclear

layer (ONL) of treated and control tissues from one individual that were embedded and cut from one block and placed consecutively on glass slides to ensure equal exposure to reagents. Measurements for content in the nuclei of Müller glia/MGPCs were made by selecting the total area of pixel values ≥70 for Sox9 immunofluorescence (in the red channel), and copying nuclear β-catenin or Pax6 (in the green channel). These copied data were pasted into a separate file for quantification or onto 70% grayscale background for figures. Measurements were made for pixels with intensity values of ≥70 (0=black and 255=saturated). The total area was calculated for clusters (≥50) of pixels above threshold. The density sum was calculated as the sum of pixel values in areas above threshold for each field of view. The average pixel intensity was calculated for all pixels within threshold regions. These calculations were performed for retinal regions sampled from at least six different retinas for each experimental condition.

Statistics

GraphPad Prism 6 was used for statistical analyses. When significance of difference was determined between two treatment groups we performed a two-way, unpaired Student's *t*-test. When significance of difference was determined between two treatment groups accounting for inter-individual variability (means of treated minus control values) we performed a two-way, paired Student's *t*-test.

Acknowledgements

The antibodies to Nkx2.2 (developed by Drs T. M. Jessell and S. Brenner-Morton), Pax6 (developed by Dr A. Kawakami) and neurofilament (developed by Dr J. Wood) were obtained from the Developmental Studies Hybridoma Bank developed under auspices of the NICHD and maintained by the University of Iowa, Department of Biological Sciences, Iowa City, IA 52242, USA.

Competing interests

The authors declare no competing or financial interests.

Author contributions

C.P.Z. designed and executed experiments, gathered data, constructed figures and contributed to writing the manuscript. L.V. designed and executed experiments, gathered data and contributed to writing the manuscript. Z.A.G. designed and executed experiments, gathered data, constructed figures and contributed to writing the manuscript. L.T. designed and executed experiments, gathered data and contributed to writing the manuscript. I.P. executed experiments, gathered data and contributed to writing the manuscript. W.A.B. executed experiments and gathered data. A.J.F. designed experiments, gathered data, constructed figures and contributed to writing the manuscript.

Funding

This work was supported by a grant [EY022030-3] from the National Eye Institute, National Institutes of Health. Deposited in PMC for release after 12 months.

Supplementary information

Supplementary information available online at
http://dev.biologists.org/lookup/suppl/doi:10.1242/dev.133215/-/DC1

References

Bernardos, R. L., Barthel, L. K., Meyers, J. R. and Raymond, P. A. (2007). Late-stage neuronal progenitors in the retina are radial Muller glia that function as retinal stem cells. *J. Neurosci.* **27**, 7028-7040.

Blackshaw, S., Harpavat, S., Trimarchi, J., Cai, L., Huang, H., Kuo, W. P., Weber, G., Lee, K., Fraioli, R. E., Cho, S.-H. et al. (2004). Genomic analysis of mouse retinal development. *PLoS Biol.* **2**, e247.

Cantrup, R., Dixit, R., Palmesino, E., Bonfield, S., Shaker, T., Tachibana, N., Zinyk, D., Dalesman, S., Yamakawa, K., Stell, W. K. et al. (2012). Cell-type specific roles for PTEN in establishing a functional retinal architecture. *PLoS ONE* **7**, e32795.

Ciuffreda, L., Incani, U. C., Steelman, L. S., Abrams, S. L., Falcone, I., Curatolo, A. D., Chappell, W. H., Franklin, R. A., Vari, S., Cognetti, F. et al. (2014). Signaling intermediates (MAPK and PI3K) as therapeutic targets in NSCLC. *Curr. Pharm. Des.* **20**, 3944-3957.

Conner, C., Ackerman, K. M., Lahne, M., Hobgood, J. S. and Hyde, D. R. (2014). Repressing Notch signaling and expressing TNFalpha are sufficient to mimic retinal regeneration by inducing Muller glial proliferation to generate committed progenitor cells. *J. Neurosci.* **34**, 14403-14419.

Dazert, E. and Hall, M. N. (2011). mTOR signaling in disease. *Curr. Opin. Cell Biol.* **23**, 744-755.

De Luca, A., Maiello, M. R., D'Alessio, A., Pergameno, M. and Normanno, N. (2012). The RAS/RAF/MEK/ERK and the PI3K/AKT signalling pathways: role in cancer pathogenesis and implications for therapeutic approaches. *Expert Opin. Ther. Targets* **16** Suppl. 2, S17-S27.

Fausett, B. V. and Goldman, D. (2006). A role for alpha1 tubulin-expressing Muller glia in regeneration of the injured zebrafish retina. *J. Neurosci.* **26**, 6303-6313.

Fischer, A. J. (2005). Neural regeneration in the chick retina. *Prog. Retin. Eye Res.* **24**, 161-182.

Fischer, A. J. and Bongini, R. (2010). Turning Muller glia into neural progenitors in the retina. *Mol. Neurobiol.* **42**, 199-209.

Fischer, A. J. and Omar, G. (2005). Transitin, a nestin-related intermediate filament, is expressed by neural progenitors and can be induced in Müller glia in the chicken retina. *J. Comp. Neurol.* **484**, 1-14.

Fischer, A. J. and Reh, T. A. (2001). Müller glia are a potential source of neural regeneration in the postnatal chicken retina. *Nat. Neurosci.* **4**, 247-252.

Fischer, A. J. and Reh, T. A. (2003). Potential of Müller glia to become neurogenic retinal progenitor cells. *Glia* **43**, 70-76.

Fischer, A. J., Pickett Seltner, R. L., Poon, J. and Stell, W. K. (1998a). Immunocytochemical characterization of quisqualic acid- and N-methyl-D-aspartate-induced excitotoxicity in the retina of chicks. *J. Comp. Neurol.* **393**, 1-15.

Fischer, A. J., Seltner, R. L. and Stell, W. K. (1998b). Opiate and N-methyl-D-aspartate receptors in form-deprivation myopia. *Vis. Neurosci.* **15**, 1089-1096.

Fischer, A. J., McGuire, C. R., Dierks, B. D. and Reh, T. A. (2002). Insulin and fibroblast growth factor 2 activate a neurogenic program in Muller glia of the chicken retina. *J. Neurosci.* **22**, 9387-9398.

Fischer, A. J., Omar, G., Eubanks, J., McGuire, C. R., Dierks, B. D. and Reh, T. A. (2004). Different aspects of gliosis in retinal Muller glia can be induced by CNTF, insulin and FGF2 in the absence of damage. *Mol. Vis.* **10**, 973-986.

Fischer, A. J., Scott, M. A., Ritchey, E. R. and Sherwood, P. (2009a). Mitogen-activated protein kinase-signaling regulates the ability of Müller glia to proliferate and protect retinal neurons against excitotoxicity. *Glia* **57**, 1538-1552.

Fischer, A. J., Scott, M. A. and Tuten, W. (2009b). Mitogen-activated protein kinase-signaling stimulates Müller glia to proliferate in acutely damaged retinas. *Glia* **57**, 1538-1552.

Fischer, A. J., Scott, M. A., Zelinka, C. and Sherwood, P. (2010). A novel type of glial cell in the retina is stimulated by insulin-like growth factor 1 and may exacerbate damage to neurons and Müller glia. *Glia* **58**, 633-649.

Fischer, A. J., Zelinka, C., Gallina, D., Scott, M. A. and Todd, L. (2014). Reactive microglia and macrophage facilitate the formation of Müller glia-derived retinal progenitors. *Glia* **62**, 1608-1628.

Fishwick, K. J., Li, R. A., Halley, P., Deng, P. and Storey, K. G. (2010). Initiation of neuronal differentiation requires PI3-kinase/TOR signalling in the vertebrate neural tube. *Dev. Biol.* **338**, 215-225.

Gallina, D., Todd, L. and Fischer, A. J. (2014a). A comparative analysis of Müller glia-mediated regeneration in the vertebrate retina. *Exp. Eye Res.* **123**, 121-130.

Gallina, D., Zelinka, C. and Fischer, A. J. (2014b). Glucocorticoid receptors in the retina, Muller glia and the formation of Muller glia-derived progenitors. *Development* **141**, 3340-3351.

Gallina, D., Palazzo, I., Steffenson, L., Todd, L. and Fischer, A. J. (2016). Wnt/βcatenin-signaling and the formation of Muller glia-derived progenitors in the chick retina. *Dev. Neurobiol.* (in press).

Ghai, K., Stanke, J. J. and Fischer, A. J. (2008). Patterning of the circumferential marginal zone of progenitors in the chicken retina. *Brain Res.* **1192**, 76-89.

Ghai, K., Zelinka, C. and Fischer, A. J. (2009). Serotonin released from amacrine neurons is scavenged and degraded in bipolar neurons in the retina. *J. Neurochem.* **111**, 1-14.

Ghai, K. Zelinka, C. and Fischer, A. J. (2010). Notch signaling influences neuroprotective and proliferative properties of mature Muller glia. *J. Neurosci.* **30**, 3101-3112.

Hamburger, V. and Hamilton, HL (1951). A series of normal stages in the development of the chick embryo. *J. Morphol.* **88**, 49-92.

Hayes, S., Nelson, B. R., Buckingham, B. and Reh, T. A. (2007). Notch signaling regulates regeneration in the avian retina. *Dev. Biol.* **312**, 300-311.

Haynes, T., Luz-Madrigal, A., Reis, E. S., Echeverri Ruiz, N. P., Grajales-Esquivel, E., Tzekou, A., Tsonis, P. A., Lambris, J. D. and Del Rio-Tsonis, K. (2013). Complement anaphylatoxin C3a is a potent inducer of embryonic chick retina regeneration. *Nat. Commun.* **4**, 2312.

Karl, M. O., Hayes, S., Nelson, B. R., Tan, K., Buckingham, B. and Reh, T. A. (2008). Stimulation of neural regeneration in the mouse retina. *Proc. Natl. Acad. Sci. USA* **105**, 19508-19513.

Kassen, S. C., Thummel, R., Campochiaro, L. A., Harding, M. J., Bennett, N. A. and Hyde, D. R. (2009). CNTF induces photoreceptor neuroprotection and Müller glial cell proliferation through two different signaling pathways in the adult zebrafish retina. *Exp. Eye Res.* **88**, 1051-1064.

Lahne, M., Li, J., Marton, R. M. and Hyde, D. R. (2015). Actin-Cytoskeleton- and Rock-Mediated INM are required for photoreceptor regeneration in the adult zebrafish retina. *J. Neurosci.* **35**, 15612-15634.

Development (2016) 143, 1859-1873 doi:10.1242/dev.133215

Lenkowski, J. R., Qin, Z., Sifuentes, C. J., Thummel, R., Soto, C. M., Moens, C. B. and Raymond, P. A. (2013). Retinal regeneration in adult zebrafish requires regulation of TGFbeta signaling. *Glia* **61**, 1687-1697.

Ma, L., Chen, Z., Erdjument-Bromage, H., Tempst, P. and Pandolfi, P. P. (2005). Phosphorylation and functional inactivation of TSC2 by Erk: implications for tuberous sclerosis and cancer pathogenesis. *Cell* **121**, 179-193.

McCabe, K. L., Gunther, E. C. and Reh, T. A. (1999). The development of the pattern of retinal ganglion cells in the chick retina: mechanisms that control differentiation. *Development* **126**, 5713-5724.

Nelson, B. R., Ueki, Y., Reardon, S., Karl, M. O., Georgi, S., Hartman, B. H., Lamba, D. A. and Reh, T. A. (2011). Genome-wide analysis of Müller glial differentiation reveals a requirement for Notch signaling in postmitotic cells to maintain the glial fate. *PLoS ONE* **6**, e22817.

Nelson, C. M., Gorsuch, R. A., Bailey, T. J., Ackerman, K. M., Kassen, S. C. and Hyde, D. R. (2012). Stat3 defines three populations of müller glia and is required for initiating maximal müller glia proliferation in the regenerating zebrafish retina. *J. Comp. Neurol.* **520**, 4294-4311.

Nelson, C. M., Ackerman, K. M., O'Hayer, P., Bailey, T. J., Gorsuch, R. A. and Hyde, D. R. (2013). Tumor necrosis factor-alpha is produced by dying retinal neurons and is required for Muller glia proliferation during zebrafish retinal regeneration. *J. Neurosci.* **33**, 6524-6539.

Ooto, S., Akagi, T., Kageyama, R., Akita, J., Mandai, M., Honda, Y. and Takahashi, M. (2004). Potential for neural regeneration after neurotoxic injury in the adult mammalian retina. *Proc. Natl. Acad. Sci. USA* **101**, 13654-13659.

Osakada, F., Ooto, S., Akagi, T., Mandai, M., Akaike, A. and Takahashi, M. (2007). Wnt signaling promotes regeneration in the retina of adult mammals. *J. Neurosci.* **27**, 4210-4219.

Paliouras, G. N., Hamilton, L. K., Aumont, A., Joppe, S. E., Barnabe-Heider, F. and Fernandes, K. J. L. (2012). Mammalian target of rapamycin signaling is a key regulator of the transit-amplifying progenitor pool in the adult and aging forebrain. *J. Neurosci.* **32**, 15012-15026.

Pardo, O. E., Arcaro, A., Salerno, G., Tetley, T. D., Valovka, T., Gout, I. and Seckl, M. J. (2001). Novel cross talk between MEK and S6K2 in FGF-2 induced proliferation of SCLC cells. *Oncogene* **20**, 7658-7667.

Parrales, A., López, E., Lee-Rivera, I. and López-Colomé, A. M. (2013). ERK1/2-dependent activation of mTOR/mTORC1/p70S6K regulates thrombin-induced RPE cell proliferation. *Cell Signal.* **25**, 829-838.

Ramachandran, R., Zhao, X.-F. and Goldman, D. (2011). Ascl1a/Dkk/beta-catenin signaling pathway is necessary and glycogen synthase kinase-3beta inhibition is sufficient for zebrafish retina regeneration. *Proc. Natl. Acad. Sci. USA* **108**, 15858-15863.

Raymond, P. A., Barthel, L. K., Bernardos, R. L. and Perkowski, J. J. (2006). Molecular characterization of retinal stem cells and their niches in adult zebrafish. *BMC Dev. Biol.* **6**, 36.

Ritchey, E. R., Zelinka, C. P., Tang, J., Liu, J. and Fischer, A. J. (2012). The combination of IGF1 and FGF2 and the induction of excessive ocular growth and extreme myopia. *Exp. Eye Res.* **99**, 1-16.

Roesch, K., Jadhav, A. P., Trimarchi, J. M., Stadler, M. B., Roska, B., Sun, B. B. and Cepko, C. L. (2008). The transcriptome of retinal Müller glial cells. *J. Comp. Neurol.* **509**, 225-238.

Rompani, S. B. and Cepko, C. L. (2010). A common progenitor for retinal astrocytes and oligodendrocytes. *J. Neurosci.* **30**, 4970-4980.

Sakagami, K., Chen, B., Nusinowitz, S., Wu, H. and Yang, X.-J. (2012). PTEN regulates retinal interneuron morphogenesis and synaptic layer formation. *Mol. Cell. Neurosci.* **49**, 171-183.

Sawyers, C. L. (2008). The cancer biomarker problem. *Nature* **452**, 548-552.

Sherpa, T., Lankford, T., McGinn, T. E., Hunter, S. S., Frey, R. A., Sun, C., Ryan, M., Robison, B. D. and Stenkamp, D. L. (2014). Retinal regeneration is facilitated by the presence of surviving neurons. *Dev. Neurobiol.* **74**, 851-876.

Stanke, J., Moose, H. E., El-Hodiri, H. M. and Fischer, A. J. (2010). Comparative study of Pax2 expression in glial cells in the retina and optic nerve of birds and mammals. *J. Comp. Neurol.* **518**, 2316-2333.

Thummel, R., Enright, J. M., Kassen, S. C., Montgomery, J. E., Bailey, T. J. and Hyde, D. R. (2010). Pax6a and Pax6b are required at different points in neuronal progenitor cell proliferation during zebrafish photoreceptor regeneration. *Exp. Eye Res.* **90**, 572-582.

Todd, L. and Fischer, A. J. (2015). Hedgehog signaling stimulates the formation of proliferating Müller glia-derived progenitor cells in the chick retina. *Development* **142**, 2610-2622.

Wan, J., Ramachandran, R. and Goldman, D. (2012). HB-EGF is necessary and sufficient for Müller glia dedifferentiation and retina regeneration. *Dev. Cell* **22**, 334-347.

Wan, J., Zhao, X.-F., Vojtek, A. and Goldman, D. (2014). Retinal injury, growth factors, and cytokines converge on beta-catenin and pStat3 signaling to stimulate retina regeneration. *Cell Rep.* **9**, 285-297.

Zelinka, C. P., Scott, M. A., Volkov, L. and Fischer, A. J. (2012). The reactivity, distribution and abundance of non-astrocytic inner retinal glial (NIRG) cells are regulated by microglia, acute damage, and IGF1. *PLoS ONE* **7**, e44477.

Zoncu, R., Efeyan, A. and Sabatini, D. M. (2011). mTOR: from growth signal integration to cancer, diabetes and ageing. *Nat. Rev. Mol. Cell Biol.* **12**, 21-35.

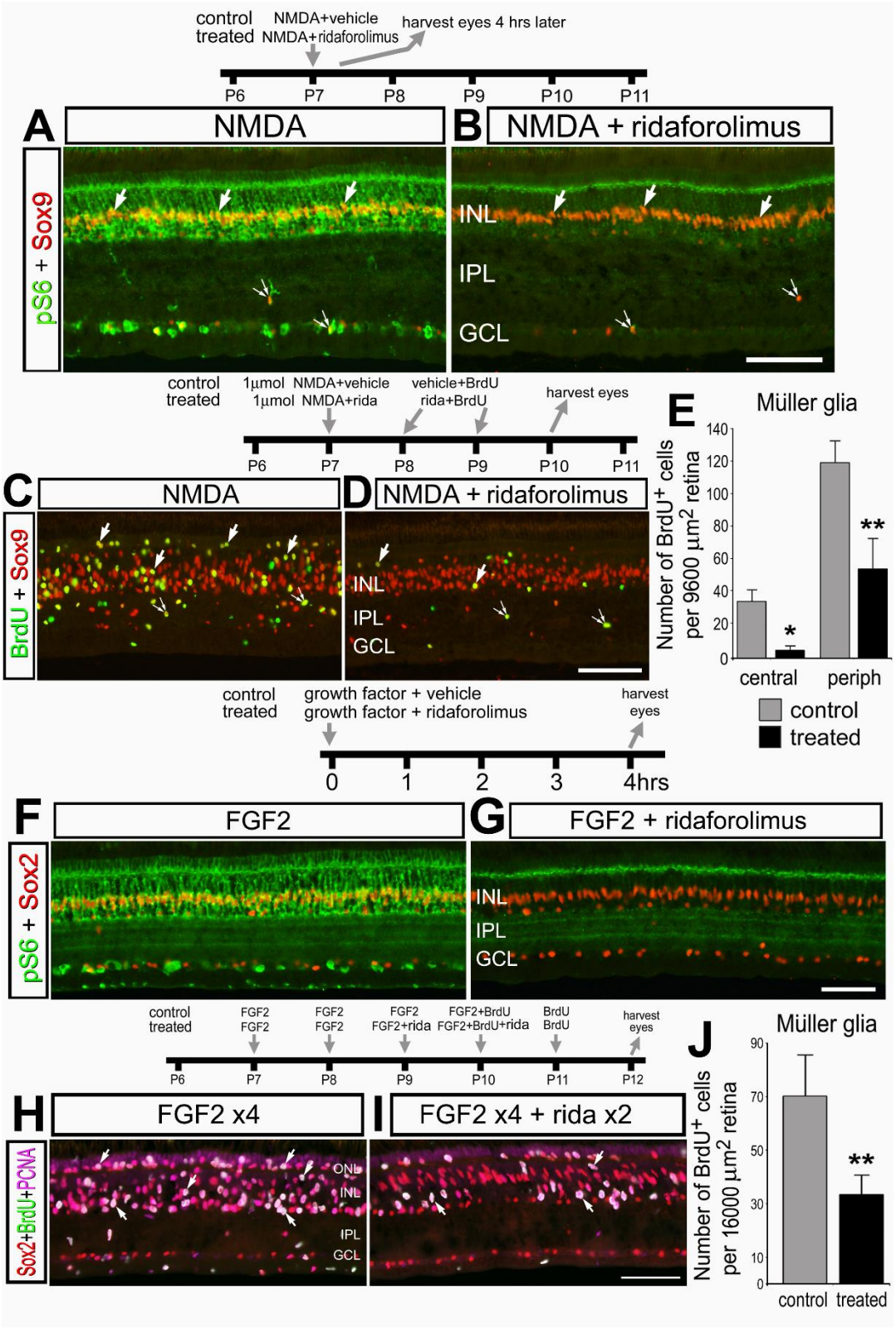

Supplemental Figure 1. Similar to the effects of rapamycin, the mTor-inhibitor ridaforolimus inhibits the induction of pS6 and the proliferation of MGPCs in NMDA-damaged and FGF2-treated retinas. The experimental paradigms are schematically

diagrammed above the relevant panels. Sections of the retina were labeled with antibodies to pS6 (green; A,B,F,G), Sox9 (red; A-D), BrdU (green; C, D, H, I), Sox2 (red; F-I), and PCNA (magenta; H, I). Arrows indicate the nuclei of Müller glia and/or MGPCs and small double-arrows indicate presumptive NIRG cells. Histograms in **E** and **J** illustrate the mean (±SD; n=4) number of proliferating Müller glia, NIRG cells and microglia in peripheral regions of control and treated retinas. Significance of difference (*p<0.05, **p<0.001) was determined by using an unpaired, two-tailed t-test. The calibration bar each panel represents 50 µm. ONL – outer nuclear layer, INL – inner nuclear layer, IPL – inner plexiform layer, GCL – ganglion cell layer.

Supplemental table 1. Antibodies, sources and working dilutions. Patterns of labeling and stimulus-dependent changes in levels of immunolabeling using these antibodies are consistent with previous reports (Fischer and Omar, 2005; Fischer et al., 2009a,b; Fischer et al., 2014; Todd and Fischer, 2015).

Antigen	**Working dilution**	**Host**	**Clone or catalog number**	**Source**
pS6	1:400	rabbit monoclonal	#5364 Ser240/244	Cell Signaling
pS6	1:750	rabbit	#2215; Ser240/244	Cell Signaling
pAkt	1:300	rabbit	#4060 Ser473	Cell Signaling
HuD/C	1:100	mouse	16A11	Invitrogen
Sox2	1:1000	goat	Y-17	Santa Cruz Immunochemicals
Brn3a (Pou4F1)	1:200	mouse	mab1585	Chemicon
neurofilament	1:50	mouse	RT97	Developmental Studies Hybridoma Bank (DSHB) Iowa City, IA
Transferrin binding protein (TFBP)	1:5000	rabbit	TFBP	Dr. J.J. Lucas, SUNY
Egr1	1:1000	goat	AF2818	R&D Systems
BrdU	1:200	rat	OBT00030S	AbD Serotec Raleigh, NC
BrdU	1:100	mouse	G3G4	DSHB
PCNA	1:1000	mouse	M0879	Dako Immunochemicals Carpinteria, CA
CD45	1:200	mouse	HIS-C7	Cedi Diagnostic
p38 MAPK	1:400	rabbit	12F8	Cell Signaling Technologies
Top_{AP}	1:100	mouse	2M6	Dr. P. Linser University of Florida
Sox9	1:2000	mouse	AB5535	Chemicon
Nkx2.2	1:80	mouse	74.5A5	DSHB
Pax6	1:50	mouse	PAX6	DSHB
Pax6	1:1000	rabbit	PRB-278P	Covance
Klf4	1:50	rabbit	ARP38430	Aviva Systems Biology

transitin	1:80	mouse	EAP3	DSHB
pERK1/2	1:200	rabbit	137F5	Cell Signaling Technologies
cFos	1:400	rabbit	K-25	Santa Cruz Immunochemicals
pCREB	1:500	rabbit	87G3	Cell Signaling Technologies

Supplemental table 2: Forward and reverse primer sequences (5' – 3') and predicted product sizes (in brackets).

Gene name	Forward	Reverse	Product size (bp)
notch1	GGC TGG TTA TCA TGG AGT TA	CAT CCA CAT TGA TCT CAC AG	(154)
hes5	GGA GAA GGA GTT CCA GAG AC	AAT TGC AGA GCT TCT TTG AG	(143)
ascl1a	AGG GAA CCA CGT TTA TGC AG	TTA TAC AGG GCC TGG TGA GC	(187)
c3aR	CACT CGC ATA TGC CAA CAG C	GCC TTT GCT CTG AAG TCC CT	(73)
c-myc	ACA CAA CTA CGC TGC TCC TC	TTC GCC TCT TGT CGT TCT CC	(154)
c3	TCC CCC ATG AGG AAT GGG AT	ATA GTC CAT GTC CCC AGG CT	(74)
gapdh	CAT CCA AGG AGT GAG CCA AG	TGG AGG AAG AAA TTG GAG GA	(161)